[AMERICAN JOURNAL OF SCIENCE, VOL. 298, JANUARY, 1998, P. 30–59]

MINERAL ZONING AND EXHUMATION HISTORY IN THE MÜNCHBERG ECLOGITES (BOHEMIA)

STÉPHANIE DUCHÊNE,* FRANCIS ALBARÈDE,*
and JEAN-MARC LARDEAUX**

ABSTRACT. Clinopyroxene and garnet from the Münchberg eclogites (Bohemia) have been analyzed by electron probe. Their zoning was examined in order to obtain information on the exhumation history of these high pressure rocks. Garnets show both growth zoning in the biggest grains and a 30 μm diffusion boundary layer. A finite-difference formulation of a volume diffusion model with a concentric arrangement of a garnet grain enclosed in a clinopyroxene matrix fails to reproduce the simultaneous existence of both zoning patterns. In contrast, exchange of Fe and Mg through the intergranular medium and transport by volume diffusion within a rock represented as an aggregate of spherical minerals account for the following general observations: (1) In most eclogites, retrograde zoning is common in garnets and absent in clinopyroxenes. (2) Retrograde zoning is restricted to garnets from high-temperature eclogites (T > 650°C). The concentration profiles depend not only on the temperature evolution but also on the respective proportions of garnet and pyroxene.

Application of the aggregate model to the Münchberg eclogites shows that the Fe-Mg profiles in the minerals are best explained by a multi-stage retrograde history in which the cooling rate decreases from $-10°C\ my^{-1}$ to $-0.5°C\ my^{-1}$ over 17.5 my. In the same interval, the exhumation rate correlatively decreases from 3 to 0.02 mm yr^{-1}. Such an evolution reflects the combination of two components of exhumation: (1) the denudation of a non-deformable crust with denudation velocity decreasing with time, and (2) the internal deformation of the crust and the existence of a vertical velocity gradient. The large value of exhumation rates at depth does not seem to be compensated by erosion which suggests a regime of intense extension in the shallow levels of the orogenic domain.

INTRODUCTION

Understanding the dynamics of orogenic phenomena amounts to reconstructing the trajectories and the velocity field of mass transport in the crust over the entire orogenic period. Structural geology strives to determine material trajectories. The velocity field must be inferred from the evolution of chemical and thermal properties in rocks and minerals that move passively with the flow. We argue elsewhere (Duchêne, Lardeaux, and Albarède, 1997) that combined thermobarometrical and geochronological data in high-pressure rocks from the Alps, the French Massif Central, and the Münchberg Massif indicate that eclogite exhumation rate decreases as their exhumation proceeds. Such an evolution may reflect two extreme tectonic regimes: (1) the denudation of a non-deformable crust with denudation velocity decreasing with time, and (2) the internal deformation of the crust which requires the existence of a vertical velocity gradient and extension at shallow level. The focus of the present work is to find independent evidence that exhumation rate decreases with time along the PT path of eclogites using the interpretation of major-element profiles in coexisting garnet-clinopyroxene pairs (Lasaga, Richardson, and Holland, 1977).

Metamorphic pyroxene, plagioclase, mica, and garnet may show chemical zoning that preserves the memory of the thermodynamic and kinetic history of their host rock. In eclogites, garnet zoning may provide information on the retrograde pressure-temperature-time (PTt) path and, hence, on the key issue of their exhumation. The distinction between two types of zoning profiles (Evans, 1965; Tracy, 1982; Ghent, 1988) is particularly clear in metamorphic garnets.

* Laboratoire de Sciences de la Terre, UMR 5570, Ecole Normale Supérieure de Lyon, 46, allée d'Italie, 69364 Lyon cedex 07, France
** Laboratoire de Pétrologie et Tectonique, UMR 5570, Université Claude Bernard Lyon I, 43, Bd du 11 Novembre 1918, 69622 Villeurbanne cedex, France

· The prograde or growth zoning (Evans, 1965; Kretz, 1974) is usually irregular for most major elements. An overall trend, however, is for Mn to decrease and Mg to increase toward the mineral rim. This zoning develops during the growth of the mineral in response to either fractionation with respect to a finite reservoir or to a change in equilibrium conditions. Garnet grows and becomes more magnesian with increasing temperature. Manganese depletion in the outer layers of the mineral reflects its progressive exhaustion in the matrix (Hollister, 1966). Garnet compositional profiles therefore record the prograde evolution of pressure and temperature associated with crystal growth and depend largely of bulk rock chemistry. (Spear and Selverstone, 1983).

· The retrograde or diffusion zoning is in essence monotonous. Magnesium decreases and Fe correlatively increases toward the rim. The restriction of strong compositional gradients to the rim of each mineral supports chemical reequilibration by intergranular exchange. This zoning forms after completion of garnet growth in response to decreasing temperature (Anderson and Buckley, 1973; Lasaga, Richardson, and Holland, 1977). Magnesium is more favorably fractionated into clinopyroxene at higher temperature (Råheim and Green, 1974; Ellis and Green, 1979). The diffusive transfer of Mg into clinopyroxene depletes Mg and correlatively increases Fe in the outermost layers of the garnet. Both the distribution of Fe and Mg between garnet and clinopyroxene and their diffusion coefficients depend on temperature. Diffusion zoning and diffusional leveling of growth zoning in garnets can therefore be used to derive the retrograde temperature-time history of the host rock (Lasaga, Richardson, and Holland, 1977; Jiang and Lasaga, 1990).

Zoning in eclogitic minerals is related to the temperature at the metamorphic climax. Growth zoning is frequent in garnets from low-temperature eclogites as in the Western Alps (Bocchio, 1995) and in the Bohemian Massif (Medaris, Jelínek, and Mísař, 1995). In contrast, diffusion zoning in garnets is only known from high-temperature eclogites ($T > 650°C$) as in the Norwegian Caledonides (Griffin, 1987; Jamveit, 1987), in Dora Maira, Western Alps (Kienast and others, 1991), and in Bohemia (Dudek and Feduiková, 1974; O'Brien, 1993; Medaris, Jelínek, and Mísař, 1995). Diffusion zoning is commonly interpreted as resulting from an exchange of Fe and Mg between garnets and omphacites (Ghent, 1988) which are the most abundant if not the only ferromagnesian minerals present in the rock. Pyroxenes, however, are generally homogeneous (Dudek and Feduiková, 1974; Jamveit, 1987; Griffin, 1987; O'Brien, 1993; Bocchio, 1995). A unique example of diffusion-zoned clinopyroxene is known from a very high-temperature (1400°–1000°C) eclogite xenolith (Sautter and Harte, 1990).

The understanding of local PTt paths in metamorphic units benefits from the comparison of Fe-Mg concentration profiles observed in minerals with simulated profiles that assume diffusional transport and an arbitrary thermal history. Numerical models involving the concentric arrangement of garnet and clinopyroxene minerals, a geometry which corresponds to an inclusion surrounded by a host mineral has been computed by Wilson and Smith (1984). Such a texture is common in undeformed or mildly deformed eclogites (Smith and others, 1982). Pyroxenes may occasionally be included in garnets and are generally small and anhedral. In contrast, garnet inclusions in pyroxenes generally consist in euhedral crystals.

Eclogites with the most common texture, in which isolated grains of garnet and pyroxene are simply aggregated to each other, have not been used to estimate cooling rates because of a lack of a numerical model of diffusional exchange relevant to this arrangement. The size of pyroxene grains usually decreases when the intensity of deformation increases. Pyroxene from strongly deformed eclogites is usually recrystallized as many small grains (van Roermund and Bolland, 1981; Lardeaux and others, 1986; Buatier and others, 1991). The garnet crystals are most commonly isolated within the pyroxene matrix.

A successful assessment of a thermal history through the modeling of Fe-Mg exchange between garnet and pyroxene depends on how well the exchange mechanism is understood. The relevance of the aggregate model is contingent on the existence of fast long-range intergranular transport. Erambert and Austreim (1993) indeed suggest that fluid circulation is responsible for the development of zoning profiles in Norwegian eclogites. If, on the contrary, equilibration is controlled by chemical exchange across the interface between minerals, a concentric arrangement is appropriate. The present work is aimed at interpreting the zoning patterns of eclogitic minerals using numerical models of Fe-Mg exchange in both the concentric and aggregate arrangements. The theory will be applied to new probe data on coexisting garnet and clinopyroxene from the Münchberg eclogites, Northeastern Bohemia. This particular choice was motivated by the occurrence of diffusion zoning overprinting growth patterns in garnets that crystallized at 650° to 700°C in association with unzoned pyroxenes (Medaris, Jelínek, and Mísař, 1995).

NUMERICAL MODELING OF DIFFUSION ZONING IN ECLOGITES

The recovery of the cooling history from retrograde zoning involves the comparison of simulated profiles with compositional data. We will now examine some theoretical aspects of these simulations.

Model Description

Garnets and pyroxenes exchange Fe and Mg during cooling. It is assumed that the crystal growth rate is more rapid than the diffusion rate (large chemical Peclet number). Diffusion associated with the prograde evolution is therefore ignored. Compositional gradient developed between the core and the rim of each mineral in response to growth zoning and changing equilibrium conditions at grain boundaries is the driving force of intragranular diffusion. We assume that diffusion of Fe is balanced by a Mg counterflow, neglecting transport of other elements such as Ca. Only one concentration variable and one interdiffusion coefficient D are needed to parameterize transport during the exchange of Fe and Mg. We assume both spherical geometry and radial symmetry. Under these conditions, Fick's Second Law states that:

$$\frac{\partial C}{\partial t} = D\left(\frac{\partial^2 C}{\partial r^2} + \frac{2}{r}\frac{\partial C}{\partial r}\right) \tag{1}$$

where C is the molar concentration of the selected species, here Mg, in mol m^{-3}, r the radial coordinate in meters, t the time in seconds, and D the diffusion coefficient in m^2 s^{-1}. The solution of this partial differential equation requires the knowledge of the initial concentration profile and two boundary conditions in each mineral. A condition of no flux being imposed at $r = 0$ by the radial symmetry, only one extra condition describing the flux of material through the surface is needed. The rim concentrations are calculated simultaneously for garnet and pyroxene assuming mass conservation and surface equilibrium. The temperature-dependent partition coefficient K_D is defined as

$$K_D = \frac{C^{Fe}_{Grt}}{C^{Mg}_{Grt}} \times \frac{C^{Mg}_{Cpx}}{C^{Fe}_{Cpx}} \tag{2}$$

where C^a_b stands for concentration of cation a in mineral b. No exact solution of Fick's equation exists with the present boundary conditions (Crank, 1975). A solution has been obtained for a constant cooling rate as a series expansion by Lasaga, Richardson, and Holland (1977). For more generality, we resort to a finite-difference solution that uses the backward scheme previously used by Wilson and Smith (1984) (see app. A for details).

The final compositional profiles depend on several parameters:

1. The initial distribution of Fe and Mg in each mineral.
2. The thermal history, expressed as a relation $T = f(t)$. A simple choice is the linear relation $T = T_0 + a\,t$, where T_0 is the initial temperature and a the cooling rate, considered as constant.
3. The preexponential term D_0 and the activation energy E_a of the diffusion coefficient D (table 1) expressed through the Arrhenius law:

$$D = D_0 \exp\left(\frac{-E_a}{RT}\right) \tag{3}$$

where R is the gas constant ($J\,mol^{-1}\,K^{-1}$). In principle, the sole Fe-Mg interdiffusion coefficient should be used. The interdiffusion and self-diffusion coefficients can be derived from each other (Darken, 1948; Chakraborty and Ganguly, 1992). Given the large uncertainties on the data, using either of the two coefficients is virtually indifferent (Medaris and Wang, 1986). The problem of the choice of the diffusion coefficient will be discussed later.

4. The preexponential term K_D^0 and the exchange free energy Q of the partition coefficient K_D (table 1):

$$K_D = K_D^0 \exp\left(\frac{Q}{RT}\right) \tag{4}$$

Q is a function of pressure and composition.

TABLE 1

Parameters governing the diffusion and partition coefficients of Fe and Mg in garnet and clinopyroxene used in the present calculations

Diffusion Coefficients				
	D_0 (m^2/s)	Q (J/mol)	Experimental Conditions	Source
Diffusion coefficients in garnet				
D_{Mg}	$5.6\ 10^{-8}$	255000	750°–900°C 2 kb	Cygan and Lasaga (1983)
D_{Mg}	$9.8\ 10^{-9}$	239000	750°–900°C 2 kb	Cygan and Lasaga (1985)
D_{Mg}	1.1E-7	253178	1100°–1480°C 14–43 kb	Chakraborty and Ganguly (1992)
D_{Fe}	6.4E-8	275144	1100°–1480°C 14–43 kb	Chakraborty and Ganguly (1992)
$D_{Fe/Mg}$	$6.11\ 10^{-4}$	344000	1150°–1330°C 30 kb	Freer (1981)
$D_{Fe/Mg}$	$0.023\ 10^{-4}$	369700	1350°–1525°C 40 kb	Elphick, Ganguly, and Loomis (1981)
$D_{Fe/Mg}$	$0.82\ 10^{-9}$	224048	1350°–1525°C 40 kb	Elphick, Ganguly, and Loomis (1985)
Diffusion coefficient in clinopyroxene				
$D_{Ca\text{-}(Mg,\,Fe)}$	$3.89\ 10^{-7}$	360870	1150°–1250°C 25 kb	Brady and Mc Allister (1983)

Equilibrium constants		
	Experimental Conditions	Source
$0.0983 \exp[(3686 + 28.35\,Pkb)/T°K]$	600°–1500°C, 20–40 kb	Råheim and Green (1974)
$0.14906 \exp[(3104X_{Ca}(Grt) + 3030 + 10.86Pkb)/T°K]$	750°–1300°C, 24–30 kb	Ellis and Green (1979)
$0.24833 \exp[(-6173\,(X_{Ca}(Grt))^2 + 6731\,X_{Ca}(Grt) + 1879 + 10\,Pkb)/T°K]$	600°–1300°C, 30 kb	Krogh (1988)

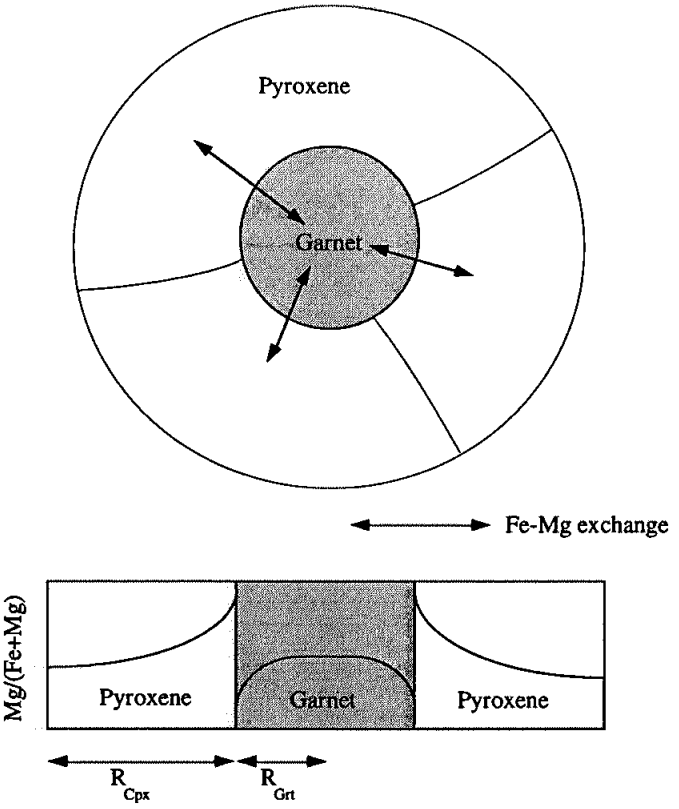

Fig. 1. Geometry of the inclusion model (model I)

5. The number of crystals of each mineral species and their radius.
6. The relative position of each crystal with respect to its neighbors.

We defined two classes of models according to the geometry (point 6) that correspond to different textures and to contrasting interpretations of the diffusion processes in mineral assemblages.

Model I: inclusion model.–The geometry of this model corresponds to a concentric inclusion/host relationship (fig. 1). The host mineral can be composed of one or more crystals. Material exchange takes place by volume diffusion across the interface between the two mineral phases. This model has previously been applied, for example, to the exchange of Fe and Mg between garnet and olivine from garnet-lherzolites (Smith and Wilson, 1985; Medaris and Wang, 1986).

Model II: population model.–In this model, analogous to the Fast Grain Boundary (FGB) model used for stable isotopes by Eiler, Baumgartner, and Valley (1992), spherical garnet and pyroxene crystals exchange cations through an intergranular medium (grain boundaries and fluids) in which diffusion is infinitely fast relative to volume diffusion in the solid phases (fig. 2).

Results

In order to understand the relative importance of the geometry and its relevant parameters, some reference simulations were first obtained using theoretical but geologi-

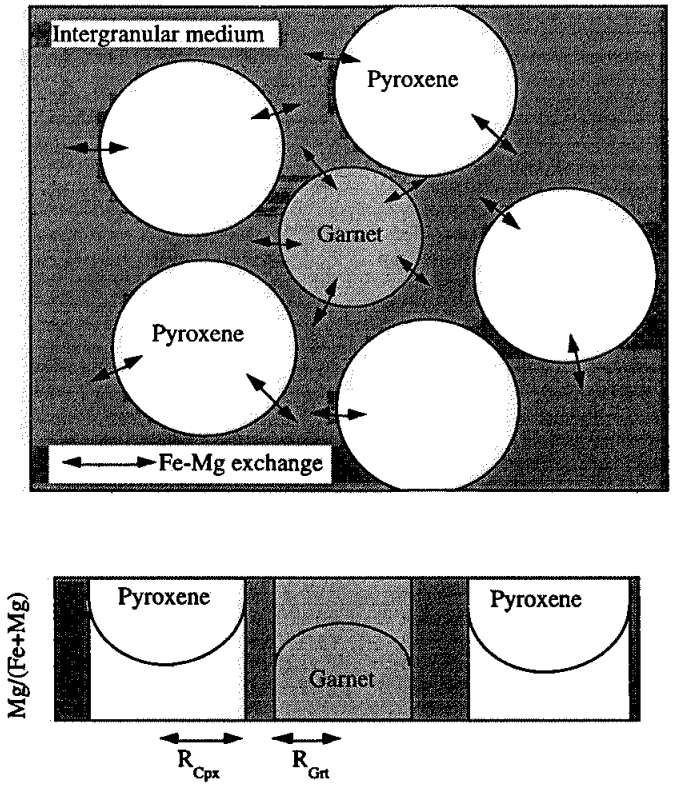

Fig. 2. Geometry of the aggregate model (model II)

cally realistic values. We selected a constant cooling rate of 2°C my^{-1} and initial temperatures of either 540 or 646°C. The temperature dependence of the equilibrium constant K_D, and the diffusion coefficients are listed in table 1.

Results for Model I.–The inclusion is represented by a spherical garnet grain of 200 μm in diameter. The surrounding pyroxene shell is 50 μm thick. The simulations show that regardless of temperature and diffusion coefficient in garnet, no significant retrograde zonation should be detected in either mineral (fig. 3). The very small value of the diffusion coefficient in pyroxene restricts transport to the outermost part of the grain, typically within 5 μm of the edge. Such a thin diffusion boundary layer would be extremely difficult to detect with the beam of an electron microprobe. Diffusion in pyroxene acting as the rate-limiting process, only a small amount of Fe and Mg will be available for exchange. In garnet, diffusion is significantly faster than in pyroxene but not fast enough for the garnet to be perfectly homogeneous. Because of the small amount of material exchanged, however, the compositional difference between the core and the rim may not be resolved by the analysis. We therefore suggest that Fe-Mg exchange by volume diffusion across the interface between concentrically arranged garnet and pyroxene cannot account for retrograde zoning in eclogitic garnets at low to medium temperature ($T < 900$°C).

Results for model II.–In contrast, the simulations (fig. 4) made on a 1:4 aggregate of garnets and pyroxenes with a radius of 200 and 350 μm, respectively, are in good

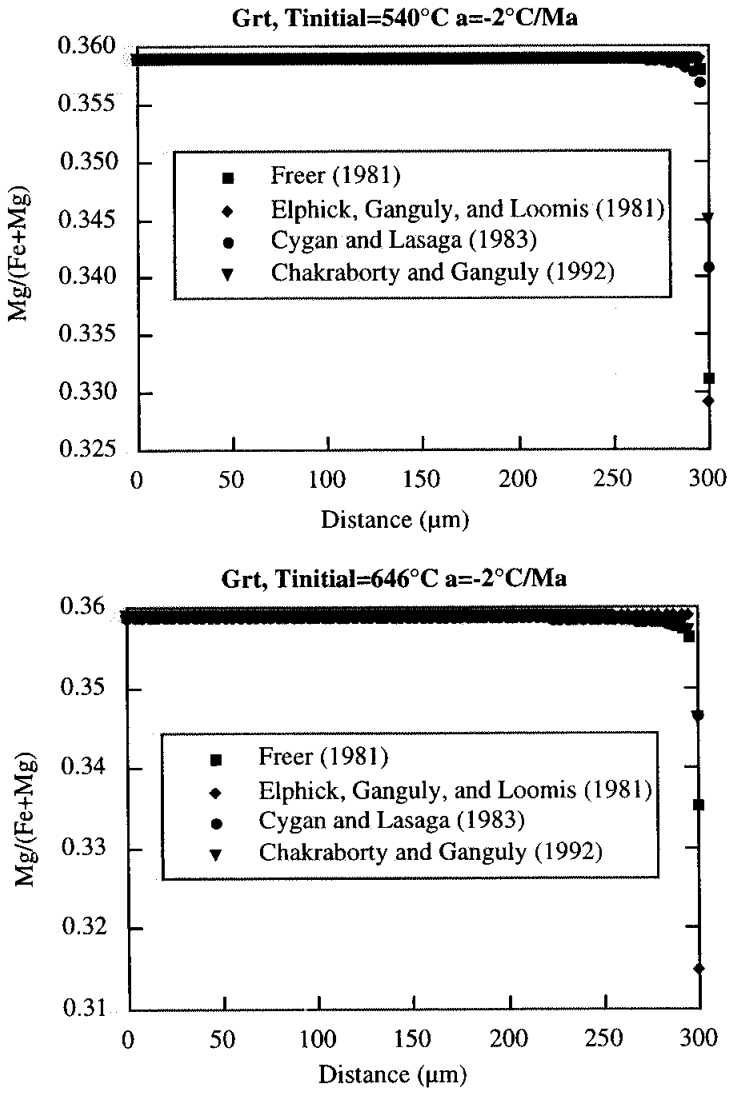

Fig. 3. Zonation profiles in garnets and clinopyroxenes simulated with inclusion model I. Four sets of diffusion coefficient parameters were tested for garnet with initial temperatures of 646° and 540°C (see text). None of these sets was able to produce zoning in garnet with an amplitude in excess of 0.2 percent. Zoning in clinopyroxene is restricted to a 2 μm boundary layer and is therefore unlikely to be detected by the microprobe.

agreement with the observations. As in Model I, the boundary layer of eclogitic pyroxenes is too thin for the zoning to be resolved by the beam of an electron microprobe. Garnets, however, are now zoned as far as the peak temperature of the metamorphism exceeds 650°C. This result is a consequence of a much larger volume of pyroxene boundary layer with respect to that of garnet, which makes more material available to volume diffusion into garnet. The effect of the volume of pyroxene boundary layer on garnet zoning is controlled by the respective values of the diffusion coefficients in each phase and can be dramatically enhanced by changing the number and the dimension of pyroxene grains (fig. 5).

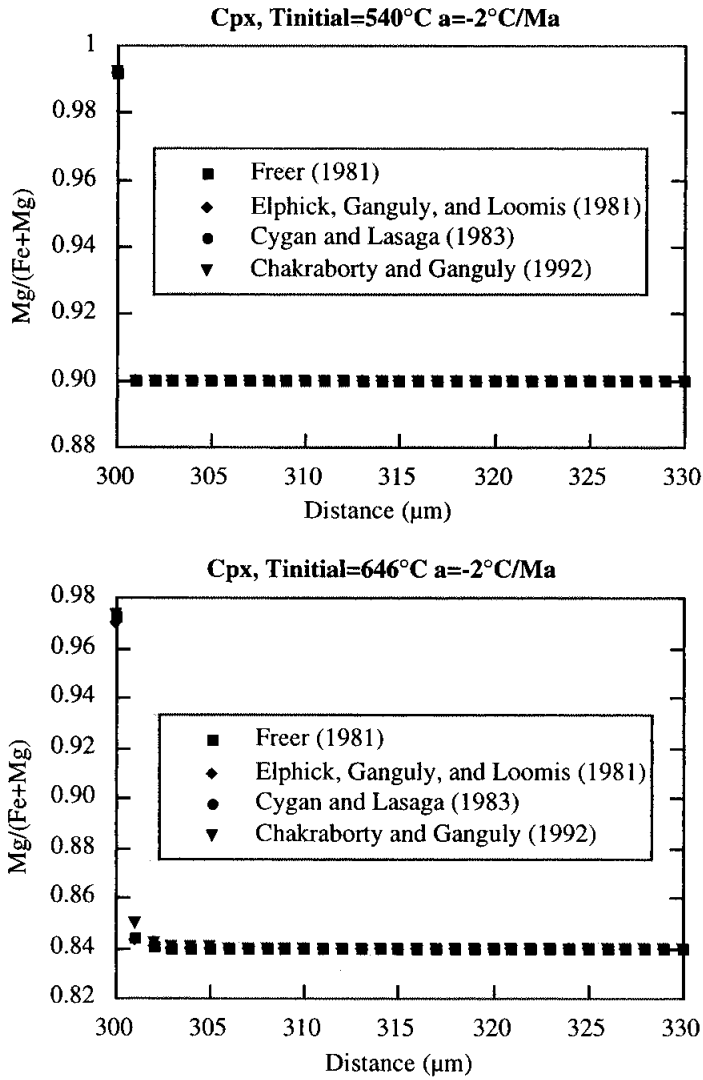

Fig. 3. (continued)

The success of this model therefore indicates that, at eclogite-facies temperatures (650°–900°C), a combination of large exchange surface area and fast intergranular transport helps cation exchanges among mineralogical phases. This model is supported by the observations of Pattison and Bégin (1994) that the thickness of the diffusion boundary layer in garnets varies by less than a factor of 2 for different adjacent minerals.

The temperatures estimated from the Fe-Mg equilibrium between garnet and clinopyroxene will depend on where in the grains the compositions are measured, but also on the texture, grain sizes, and geometry. The temperature recoverable from clinopyroxene-garnet assemblages will therefore be lower

1. for smaller grain size at constant proportions of garnet and clinopyroxene when that size approaches the thickness of the diffusion boundary layer;

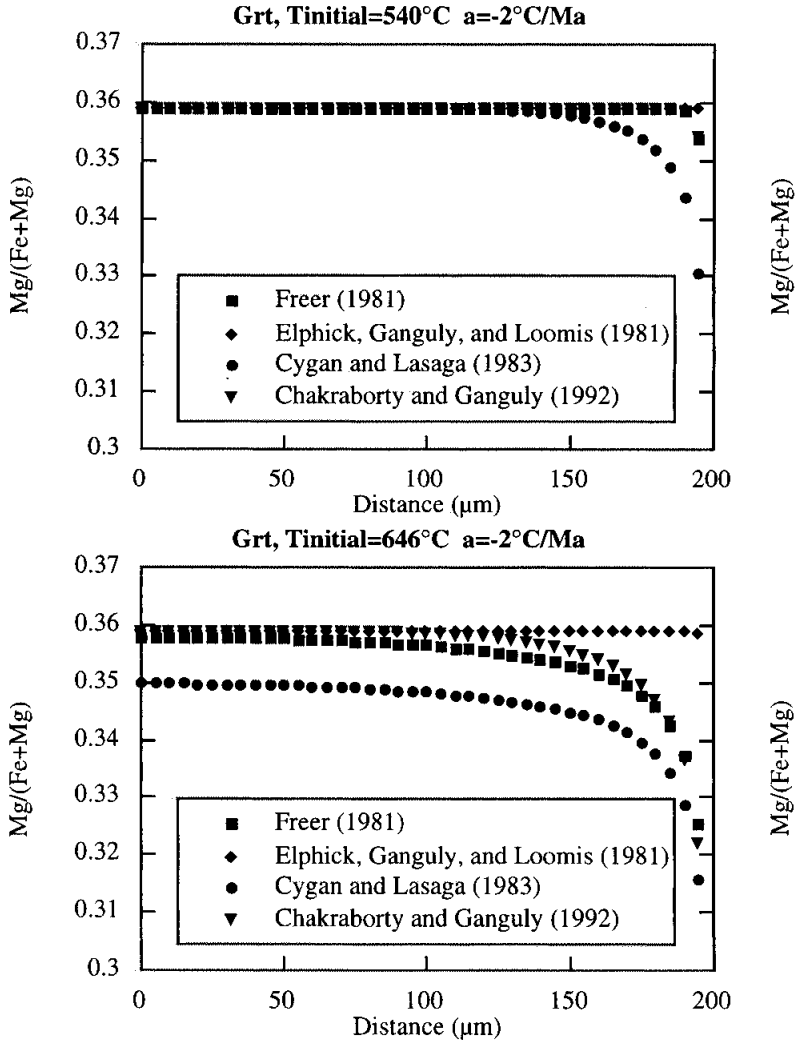

Fig. 4. Zonation profiles in garnets and clinopyroxenes simulated with aggregate model II. The aggregate is represented by one garnet grain of 200 μm in radius and four pyroxene grains of 350 μm in radius. The sets of diffusion and partition coefficient parameters and the initial temperature are the same as in figure 3. Three sets produce significant zoning in garnet at 650°C. As for model I, zoning in clinopyroxene will not be detected by the microprobe.

2. for smaller garnet/clinopyroxene ratio at constant grain sizes.

Point (1) is explicit in the formulation of closure temperature for radiogenic and stable isotopes by Dodson (1973) and Giletti (1986) while the effect of modal abundance expressed by point (2) appears in the models of oxygen isotope equilibration in cooling assemblages of Jenkin (1994) and Eiler, Baumgartner, and Valley (1992).

APPLICATION TO THE MÜNCHBERG ECLOGITES

Geological Setting

The Münchberg area (fig. 6), located in the northwestern Bohemian Massif (Bavaria, Germany), belongs to the internal zone of the European Paleozoic Belt. It is considered

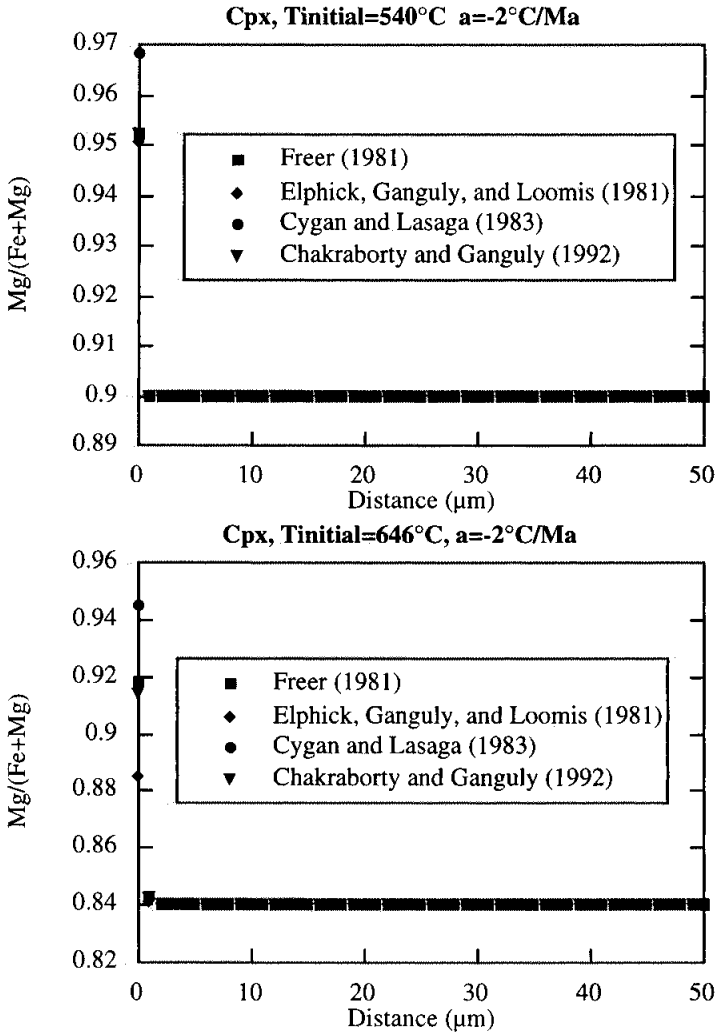

Fig. 4. (continued)

as a nappe pile with five allochtonous units of Paleozoic metasediments and metavolcanics (Behr, Engel, and Franke, 1982; Franke, 1984). The overall metamorphic grade increases from the bottom to the top of the pile: low-grade (Randschiefer Serie), greenschist facies (Prasinite-Phyllite Series), amphibolite facies (Randamphibolite-, Liegend-, and Hangend- series). Eclogitic bodies are found at the base of the uppermost Hangendserie. They occur as isolated lumps in amphibolite facies metasedimentary gneisses and mafic amphibolites. The whole Hangendserie unit is a volcaniclastic sequence that went through an early high-pressure metamorphic episode then through a retrogression is in the amphibolite facies.

Sample Description and Mineralogical Data

The samples studied are nearly bimineralic eclogites (fig. 7). Garnet and clinopyroxene occur as large euhedral grains (up to 4 mm). The garnets are homogeneously

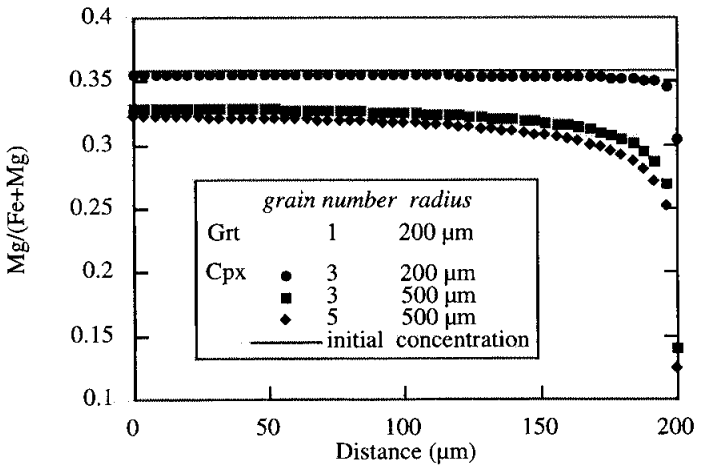

Fig. 5. Influence of the size and number of garnet and clinopyroxene grains on the zoning profile in garnet for an initial temperature of 711°C and a cooling rate a of -2°C my^{-1}.

distributed in the pyroxene matrix. Rutile, uncommon white mica, and quartz occur as accessory minerals. Inclusions of quartz, rutile, and clinopyroxene are occasionally found in garnets. Retrogressive features are infrequent and restricted to narrow symplectites of plagioclase and clinopyroxene along rare veins indicative of fluid infiltration.

The mineral compositions were measured on the electron probes of the University of Clermont-Ferrand (Camebax Micro) and of the ETH in Zürich (Camebax SX 50) using an acceleration voltage of 15 kV and a beam intensity of 20 nA. Natural oxides were used as standards. The results are presented in table 2 and in figure 8. Garnets are rich in Fe and Mg, moderately calcic, and Mn-poor ($X_{Fe^{2+}} = 0.4$-0.55, $X_{Mg} = 0.25$-0.40, $X_{Ca} = 0.18$-0.25, $X_{Mn} < 0.01$). The $X_{Fe^{3+}}$ (≈ 0.01) values were calculated assuming stoichiometry and charge equilibrium. The composition of clinopyroxenes is omphacitic with 40 to 50 percent jadeite. By contrast with the garnets, their Fe^{3+} content calculated assuming stoichiometry and charge equilibrium is negligible.

Zoning Patterns

The composition profiles have been determined in several garnet-pyroxene pairs from symplectite-free domains. The selected garnets are nearly free of inclusions and cracks and surrounded in sharp contact by pyroxene grains. The profiles in pyroxenes and garnets are in continuity across the grain boundaries.

Retrograde zoning is observed in most garnet rims (fig. 8) and is confined to the outermost 30 μm of the garnet crystals. This is consistent with the retrograde zoning profiles presented by O'Brien (1993) for Münchberg eclogites.

Prograde zoning is common in garnet cores, especially those from grains with a radius >250 μm. Zoning is strong and particularly frequent for calcium. In the smallest grains, prograde zoning is absent. As shown by O'Brien (1993), some prograde zoning patterns result from the overgrowth and coalescence of individual crystals. Occasionally, garnets present a concentric arrangement with a homogeneous core surrounded by a growth-zoned envelope (fig. 8, sample M8, site 7). The homogeneity of the smallest grains therefore suggests either that growth zoning has been erased by diffusion or that these grains represent an early generation of homogeneous garnets.

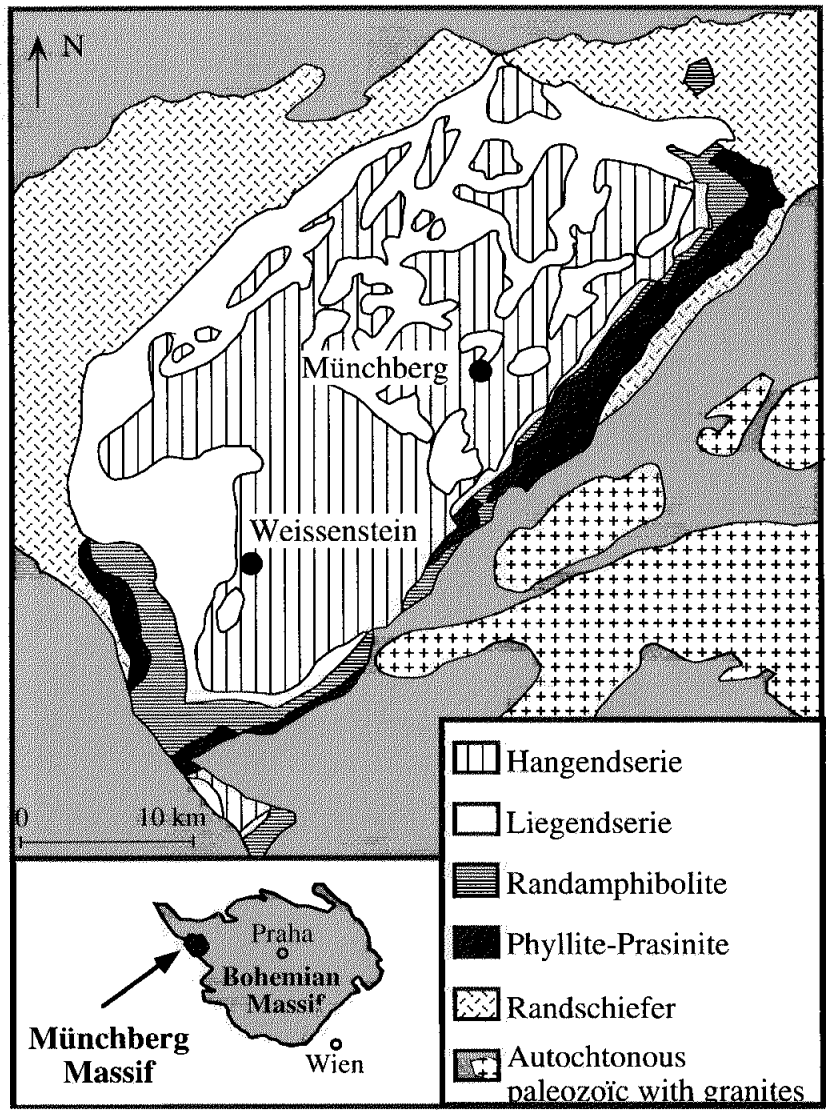

Fig. 6. Sketch map of the geology of the Münchberg Massif (after O'Brien, 1993). Samples have been collected in the locality of Weissenstein, at the base of the Hangendserie.

No retrograde pattern is observed in pyroxenes in the vicinity of garnet grain boundaries. It is a common observation in eclogites that pyroxenes are essentially homogeneous.

Previous Work on the Pressure-Temperature History of the Münchberg Eclogites

Several investigations dealing with the pressure-temperature history of the Münchberg eclogites found maximum temperatures of 600° to 700°C for the eclogitic stage using the thermometers of Ellis and Green (1979) and Krogh (1988) for garnet-clinopyroxene and that of Green and Helmann (1982) for garnet-phengite (Franz,

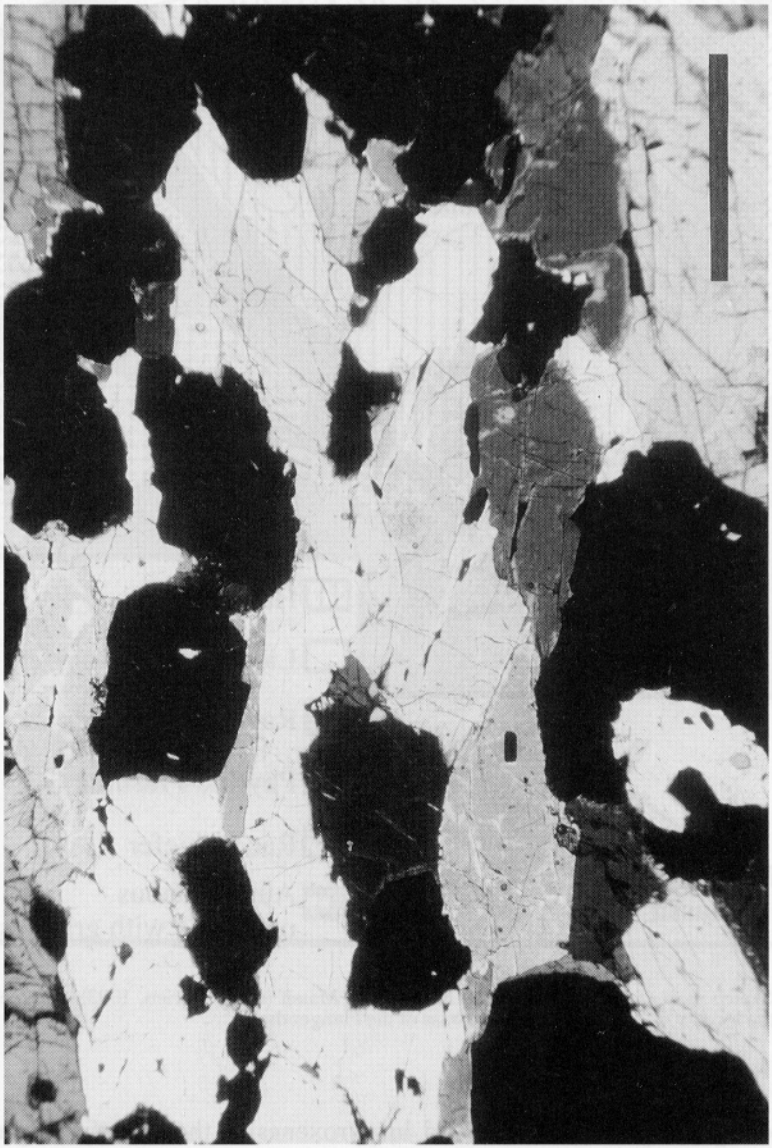

(A)

Fig. 7.

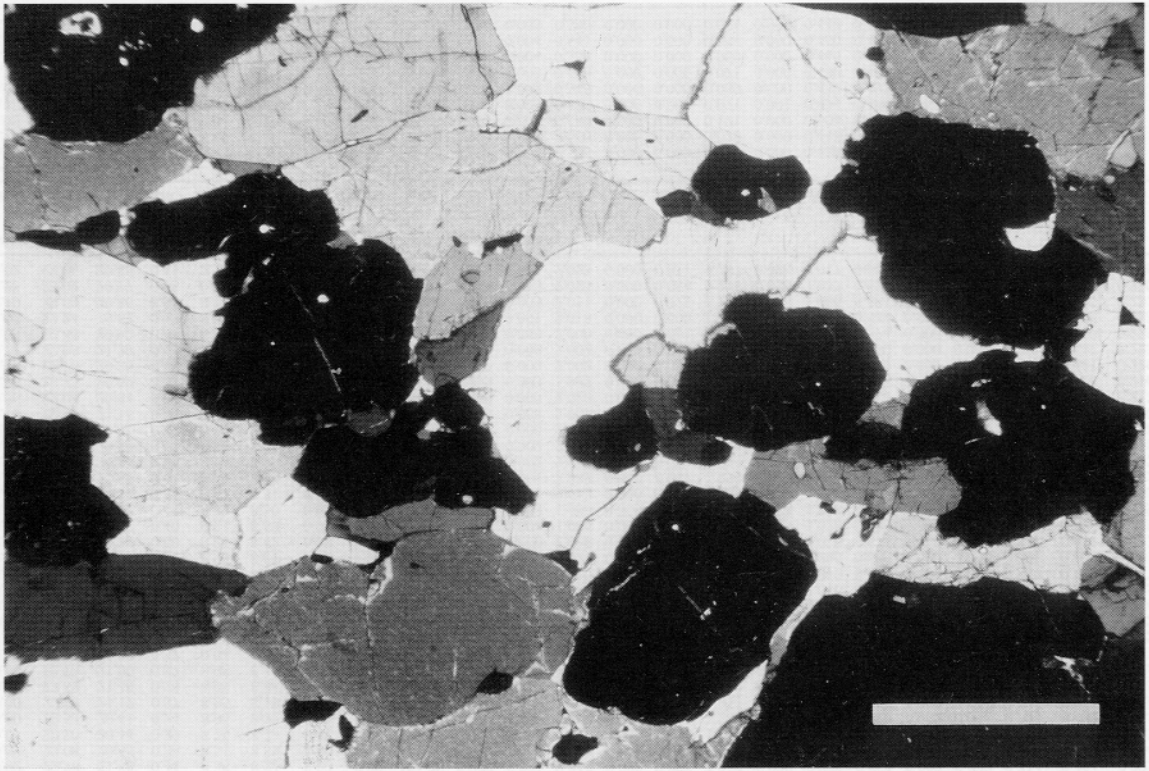

(B)

Fig. 7. Photomicrographs in cross polar of thin sections from samples (A) M8 and (B) M10. Three of the zoning profiles presented in figure 8 correspond to garnets and clinopyroxenes from sample M8, and two of them to garnets and pyroxenes from sample M10. Scale bar: 1 mm.

TABLE 2

Microprobe analysis of garnet and clinopyroxene crystals

GARNETS

	SiO2	TiO2	Al2O3	FeO	MnO	MgO	CaO	Na2O	K2O	Total	Si	Ti	Al	Cr	Fe3	Fe2	Mn	Mg	Ca	Na	K	XMg	XFe2+	XCa	XMn	Mg#
Sample M8, site 1 Δr = 5μm																										
rim	39.80	0.02	22.78	21.68	0.44	8.38	8.24	0.00	0.02	101.36	2.989	0.001	2.017	0.000	0.005	1.357	0.028	0.938	0.663	0.000	0.002	0.314	0.454	0.222	0.009	0.409
	40.79	0.09	23.08	20.55	0.36	8.51	8.59	0.00	0.00	101.97	3.037	0.005	2.026	0.000	0.000	1.280	0.023	0.945	0.685	0.000	0.000	0.322	0.436	0.234	0.008	0.425
	40.21	0.07	23.20	20.44	0.29	8.75	8.79	0.02	0.00	101.78	2.994	0.004	2.036	0.000	0.000	1.273	0.018	0.971	0.701	0.003	0.000	0.328	0.429	0.237	0.006	0.433
	39.86	0.00	22.53	20.41	0.24	8.96	8.32	0.01	0.04	100.37	3.007	0.000	2.004	0.000	0.000	1.288	0.015	1.008	0.673	0.002	0.004	0.338	0.432	0.225	0.005	0.439
	40.52	0.00	23.20	21.17	0.37	8.95	8.19	0.02	0.01	102.42	3.000	0.000	2.026	0.000	0.000	1.311	0.023	0.987	0.650	0.002	0.001	0.332	0.441	0.219	0.008	0.430
	40.37	0.05	23.52	21.48	0.28	8.98	8.44	0.00	0.07	103.18	2.967	0.003	2.038	0.000	0.030	1.290	0.017	0.984	0.665	0.001	0.006	0.333	0.436	0.225	0.006	0.433
	40.45	0.04	22.78	21.00	0.37	8.98	8.45	0.00	0.00	102.11	3.005	0.002	1.995	0.000	0.000	1.305	0.023	0.995	0.675	0.000	0.000	0.332	0.435	0.225	0.008	0.433
	40.02	0.06	23.38	20.98	0.37	9.04	8.28	0.00	0.00	102.13	2.969	0.003	2.045	0.000	0.010	1.292	0.023	1.000	0.658	0.000	0.000	0.336	0.435	0.221	0.008	0.436
	39.82	0.02	23.20	20.72	0.50	9.13	8.23	0.02	0.03	101.67	2.965	0.001	2.037	0.000	0.037	1.253	0.031	1.013	0.657	0.003	0.003	0.343	0.424	0.222	0.011	0.447
	39.95	0.10	23.16	20.57	0.42	9.07	8.28	0.01	0.00	101.55	2.979	0.005	2.036	0.000	0.000	1.282	0.026	1.008	0.661	0.002	0.000	0.339	0.431	0.222	0.009	0.440
	39.84	0.06	23.10	20.69	0.43	8.95	8.29	0.03	0.05	101.44	2.975	0.003	2.034	0.000	0.017	1.275	0.027	0.996	0.663	0.004	0.005	0.336	0.431	0.224	0.009	0.439
	40.01	0.03	23.19	20.58	0.32	9.10	8.39	0.00	0.03	101.65	2.979	0.001	2.036	0.000	0.007	1.275	0.020	1.010	0.669	0.000	0.003	0.339	0.429	0.225	0.007	0.442
	39.94	0.12	22.98	21.09	0.39	9.11	8.09	0.00	0.00	101.70	2.977	0.007	2.019	0.000	0.013	1.302	0.024	1.012	0.646	0.000	0.000	0.339	0.436	0.217	0.008	0.437
	40.13	0.03	23.05	20.47	0.30	8.95	8.61	0.00	0.00	101.53	2.993	0.002	2.027	0.000	0.000	1.277	0.019	0.995	0.688	0.000	0.000	0.334	0.439	0.231	0.006	0.438
	39.88	0.00	23.24	20.39	0.40	9.26	8.42	0.03	0.01	101.62	2.966	0.000	2.038	0.000	0.035	1.233	0.025	1.026	0.671	0.004	0.001	0.347	0.417	0.227	0.009	0.454
	39.88	0.07	22.55	20.77	0.40	9.21	8.53	0.00	0.01	101.41	2.979	0.004	1.986	0.000	0.050	1.247	0.025	1.025	0.683	0.000	0.001	0.344	0.418	0.229	0.008	0.451
	39.93	0.06	22.76	20.72	0.44	9.32	8.50	0.02	0.01	101.76	2.970	0.003	1.996	0.000	0.062	1.227	0.028	1.033	0.678	0.003	0.001	0.348	0.414	0.229	0.009	0.457
	39.81	0.02	22.82	20.24	0.35	9.27	8.51	0.01	0.00	101.02	2.979	0.001	2.013	0.000	0.029	1.238	0.022	1.034	0.682	0.002	0.000	0.347	0.416	0.229	0.007	0.455
	39.28	0.03	22.87	20.57	0.41	9.13	8.13	0.01	0.00	100.43	2.960	0.002	2.032	0.000	0.047	1.250	0.026	1.025	0.657	0.002	0.000	0.347	0.423	0.222	0.009	0.451
	39.45	0.04	23.05	20.84	0.29	9.14	7.99	0.00	0.02	100.83	2.962	0.002	2.041	0.000	0.034	1.275	0.019	1.023	0.643	0.000	0.002	0.346	0.431	0.217	0.006	0.445
	39.61	0.04	23.17	20.53	0.41	9.35	8.04	0.02	0.01	101.20	2.959	0.002	2.041	0.000	0.041	1.242	0.026	1.041	0.644	0.003	0.001	0.353	0.421	0.218	0.009	0.456
	39.71	0.11	22.88	20.81	0.42	9.49	8.48	0.00	0.00	101.89	2.948	0.006	2.003	0.000	0.089	1.203	0.026	1.050	0.674	0.000	0.000	0.355	0.407	0.228	0.009	0.466
	40.20	0.14	22.97	21.15	0.36	9.18	8.27	0.02	0.00	102.29	2.979	0.008	2.007	0.000	0.023	1.287	0.022	1.014	0.656	0.003	0.000	0.340	0.432	0.220	0.008	0.441
	39.71	0.06	22.94	20.84	0.28	9.30	8.02	0.03	0.00	101.17	2.970	0.003	2.022	0.000	0.036	1.268	0.018	1.037	0.643	0.004	0.000	0.350	0.428	0.217	0.006	0.450
	40.38	0.06	22.75	20.69	0.33	9.45	8.08	0.08	0.00	101.82	2.999	0.003	1.992	0.000	0.015	1.270	0.021	1.045	0.643	0.012	0.000	0.351	0.426	0.216	0.007	0.452
	39.90	0.00	22.76	20.36	0.48	9.37	8.38	0.06	0.00	101.32	2.977	0.000	2.002	0.000	0.054	1.217	0.030	1.042	.0670	0.009	0.000	0.352	0.411	0.226	0.010	0.461
	39.90	0.11	22.95	21.29	0.43	9.42	8.32	0.00	0.00	102.41	2.951	0.006	2.002	0.000	0.084	1.233	0.027	1.038	0.659	0.000	0.000	0.351	0.417	0.223	0.009	0.457
	39.81	0.05	22.85	20.92	0.37	9.39	8.47	0.04	0.01	101.90	2.955	0.003	2.000	0.000	0.091	1.208	0.023	1.039	0.674	0.006	0.001	0.353	0.410	0.229	0.008	0.462
	39.64	0.02	22.24	19.62	0.48	8.35	7.83	0.35	0.00	98.54	3.043	0.001	2.013	0.000	0.000	1.260	0.031	0.955	0.644	0.053	0.000	0.331	0.436	0.223	0.011	0.431
	39.93	0.10	23.03	20.86	0.56	9.11	8.58	0.05	0.04	102.24	2.958	0.005	2.011	0.000	0.072	1.221	0.035	1.006	0.681	0.007	0.004	0.342	0.415	0.231	0.012	0.452
	39.51	0.23	23.02	20.27	0.48	9.33	8.50	0.00	0.02	101.35	2.949	0.013	2.025	0.000	0.054	1.211	0.030	1.037	0.679	0.000	0.002	0.351	0.409	0.230	0.010	0.461
core	40.11	0.02	23.06	20.86	0.41	9.17	8.05	0.02	0.04	101.74	2.986	0.001	2.023	0.000	0.011	1.287	0.026	1.017	0.642	0.003	0.004	0.342	0.433	0.216	0.009	0.441

Formulae were calculated on the basis of 12 oxygenes and Fe3+ estimated by charge balance

PYROXENE

	SiO2	TiO2	Al203	FeO	MnO	MgO	CaO	Na2O	K2O	Total	Si	Ti	Al	Cr	Fe3	Fe2	Mn	Mg	Ca	Na	K	XMg
M8 site 1 Δr = 4 μm																						
rim	56.40	0.13	12.60	2.25	0.00	8.33	12.93	7.04	0.01	99.69	1.993	0.004	0.525	0.000	0.000	0.067	0.000	0.439	0.490	0.482	0.000	0.868
	55.31	0.13	13.12	2.62	0.00	8.45	12.61	6.91	0.00	99.15	1.965	0.003	0.550	0.000	0.000	0.078	0.000	0.448	0.480	0.476	0.000	0.852
	50.79	0.05	13.34	5.70	0.00	9.04	10.64	5.46	0.06	95.08	1.901	0.001	0.589	0.000	0.007	0.171	0.000	0.504	0.427	0.396	0.004	0.747
	56.54	0.13	13.05	2.41	0.03	8.31	12.88	7.13	0.02	100.49	1.982	0.003	0.539	0.000	0.000	0.071	0.001	0.434	0.484	0.485	0.001	0.860
	56.32	0.07	13.15	2.35	0.00	8.34	13.03	7.01	0.00	100.28	1.979	0.002	0.545	0.000	0.000	0.069	0.000	0.437	0.491	0.478	0.000	0.863
	56.66	0.13	13.03	2.42	0.01	8.43	13.12	7.12	0.02	100.92	1.978	0.003	0.536	0.000	0.000	0.071	0.000	0.439	0.491	0.482	0.001	0.861
	56.78	0.14	12.98	2.03	0.00	8.49	12.79	6.94	0.03	100.19	1.996	0.004	0.538	0.000	0.000	0.060	0.000	0.445	0.482	0.473	0.002	0.881
	56.43	0.17	13.08	2.19	0.02	8.60	12.84	7.01	0.00	100.33	1.980	0.004	0.541	0.000	0.000	0.064	0.000	0.450	0.483	0.477	0.000	0.875
	56.40	0.11	12.95	2.16	0.00	8.57	12.91	7.10	0.01	100.21	1.980	0.003	0.536	0.000	0.000	0.064	0.000	0.448	0.485	0.483	0.001	0.876

Formulae were calculated on the basis of 6 oxygenes

Matthes, and Okrusch, 1986; Klemd, 1989; Klemd, Thomas, and Smith, 1991a; O'Brien, 1993) (fig. 9).

Applying the Fe^{2+}/Mg exchange thermometry to the rims of pyroxenes and adjacent garnets, we find temperatures of 650° to 700° (table 3). If cores are used in place of rims, the temperatures tend to cluster in the upper part of that range, which in the less growth-zoned garnets reflects the diffusion effects in the garnet rims (samples M10 site 2, M8 site 1 and 3). The highest temperatures were obtained using the garnet-clinopyroxene thermometer of Ellis and Green (1979).

The minimum pressure calculated for the eclogite-facies metamorphism from the jadeite content of omphacites in the presence of quartz or from the composition of phengites is 15 ± 2 kb (Franz, Thomas, and Smith, 1986; O'Brien, 1993). O'Brien (1993) estimated that the presence of kyanite-paragonite-jadeite and grossular-zoisite-kyanite-quartz assemblages require significantly higher pressures of 20 to 25 kb.

The Rb-Sr mineral isochrons of Söllner (1978) and Stosch and Lugmair (1990) and the U-Pb data on zircons of Gebauer and Grünenfelder (1979) indicate consistent ages of 370 to 395 Ma for the eclogitic stage. The retrograde path is assumed to have begun with a nearly isothermal decompression (large dP/dT) which ended in the amphibolite facies 365 to 390 Ma ago (Söllner, Köhler, and Müller-Sohnius, 1981; Schüssler and others, 1986; Kreutzer and Seidel, 1989; Kreutzer and others, 1989). The PT path at shallow depth reflects nearly isobaric cooling (large dT/dP) and crosses the prehnite-pumpellyite facies at 300 Ma (Hammerschmidt and Franz, 1992).

Modeling of Münchberg Zoning

We used Model II to simulate the zoning patterns of the Münchberg eclogitic minerals. The simulations are expected to account for (1) the thickness of the diffusion boundary layer, (2) the amplitude of retrograde zoning, (3) the preservation of prograde growth-zoning, the details of which are virtually immaterial to the estimated cooling rates (Jiang and Lasaga, 1990).

We estimated the relative abundance of garnets and pyroxenes from the number of pixels associated with each mineral species on digitized microphotographs. On average, the Münchberg eclogites contain 30 percent garnet and 70 percent pyroxene, and the variability of these figures is small on the scale of a thin section. A typical assemblage selected for the present study would consist of one garnet and three pyroxene crystals with a same radius of about 250 μm.

As for the reference models, we used the equilibrium constant K_D of Ellis and Green (1979), which gives a 650°C rim temperature consistent with the peak temperature admitted by Franz, Thomas, and Smith (1986), Klemd (1989), and O'Brien (1993).

Garnet diffusion coefficients have been reported by different groups (fig. 10) and, once corrected for oxygen fugacity, agree within better than two orders of magnitude. Freer (1981) and Elphick, Ganguly, and Loomis (1985) reported Fe-Mg inter-diffusion measurements while Cygan and Lasaga (1983, 1985) dealt with Mg self-diffusion. The more recent results for Mg and Fe self-diffusion by Chakraborty and Ganguly (1992) take a wide range of temperature, pressure, and garnet composition under controlled oxygen fugacity into account. We used this latter set which enables the diffusion coefficient to be precisely evaluated for variable compositions along the decompression path. At 14.5 kb, the activation energy Ea is higher by 8000 J and the diffusion coefficient half an order of magnitude smaller than at 1 bar, a difference significantly less than the range of diffusion coefficients at a given temperature reported by different laboratories. To evaluate the uncertainties on cooling rates introduced by different sets of diffusion coefficients, we also evaluated some solutions using the more 'rapid' data of Freer (1981). In the absence of the relevant data, Ca in both clinopyroxene and garnet was assumed to be immobile.

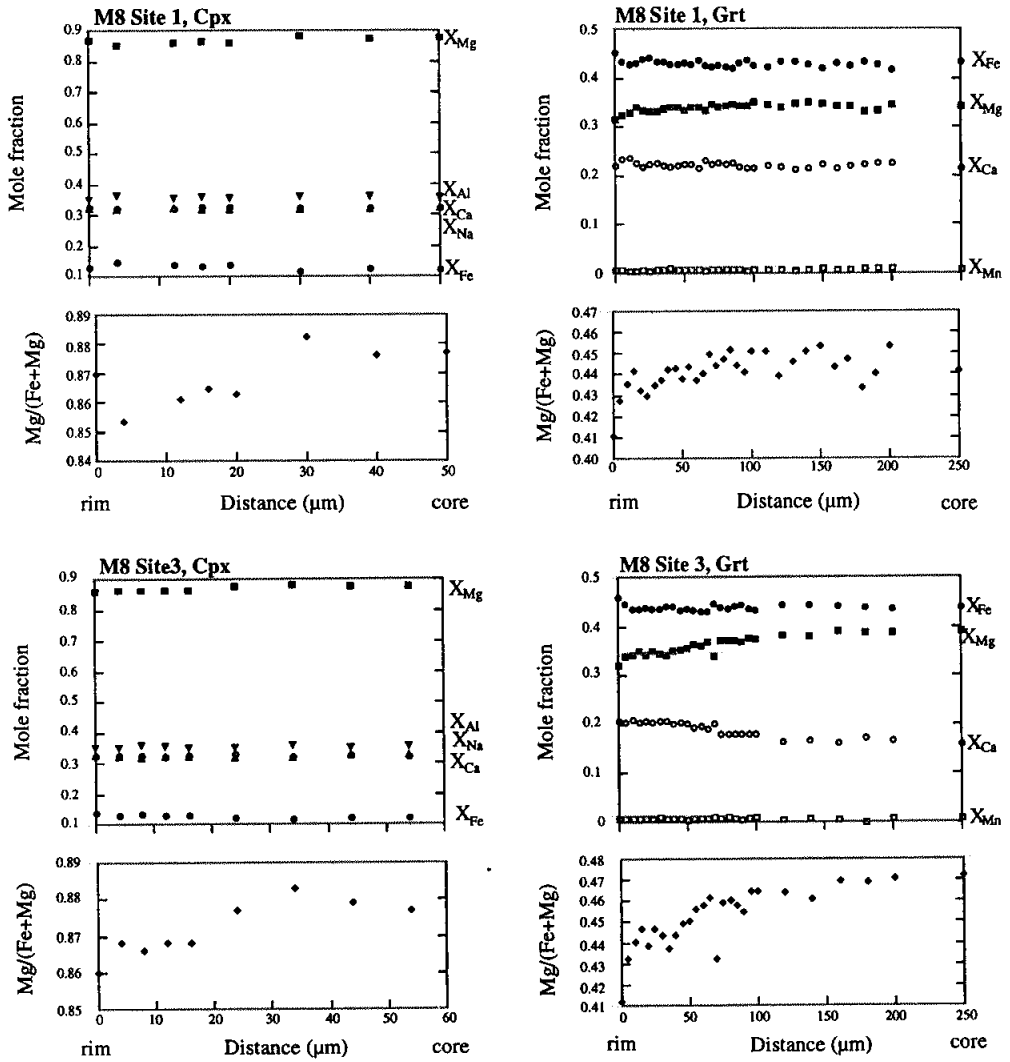

Fig. 8. Zoning profiles across adjacent crystals of garnet and clinopyroxene. Typical microprobe analyses are reported in table 2. Δr is the distance between two analytic points.

The Fe-Mg diffusion coefficient was approximated by Brady and MacAllister's (1983) Ca-Mg interdiffusion values.

Temperature-time History

Twelve temperature-time functional relationships were selected. Six relations are linear temperature-time functions, with cooling rates in the range 1° to 30°C my^{-1}. The other six relations represent 3-stage histories, with stepwise-constant cooling rates, either decreasing or increasing through time. Zoning profiles were calculated for each model, first on initially homogeneous garnets, second on growth-zoned garnets with arbitrarily

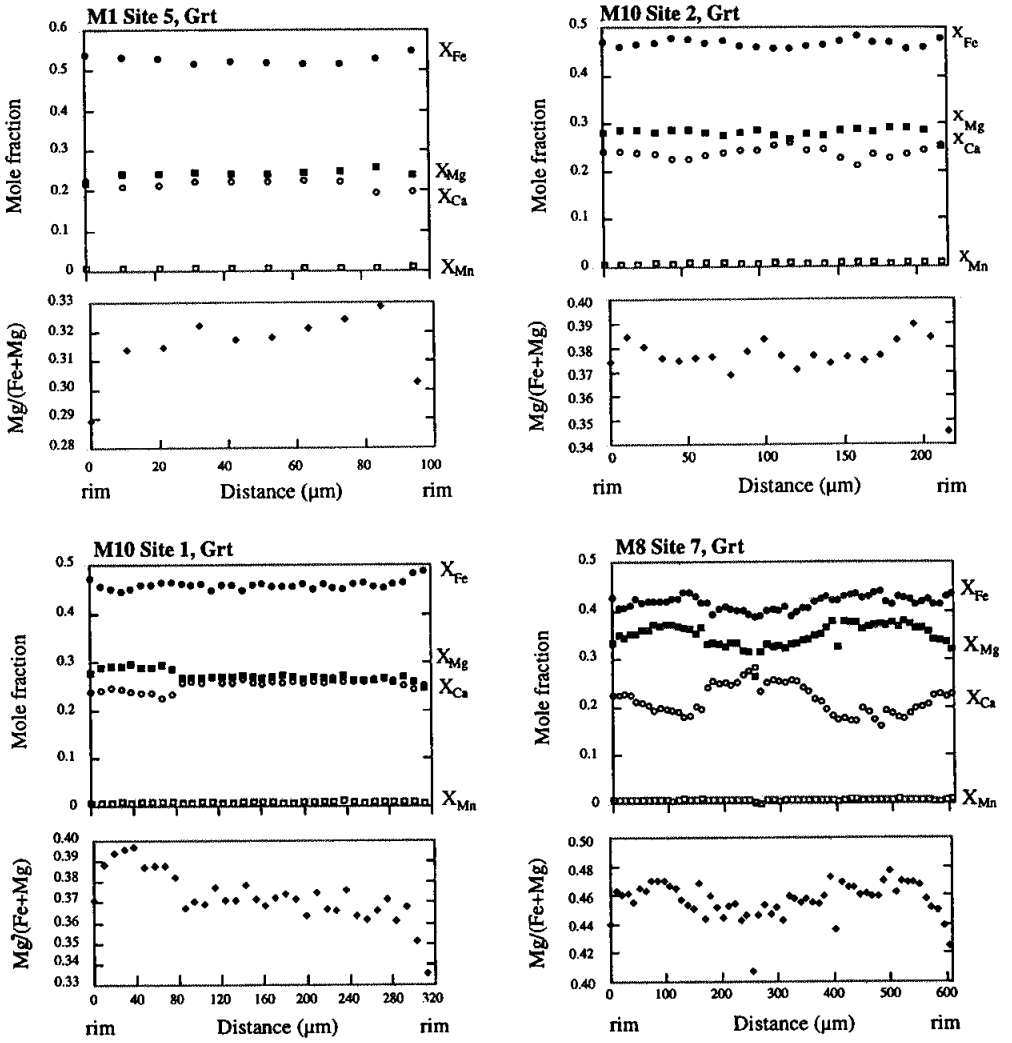

Fig. 8 (continued)

defined profiles. The size and surface composition of the garnets correspond to those found in six actual crystals from the Münchberg eclogites. The corresponding peak temperatures range from 650° to 700°C and reflect therefore the uncertainty on the temperature of the metamorphism. The results for three of these garnet crystals and selected temperature-time relationship are shown on figure 11.

A first set of numerical experiments was conducted assuming a constant cooling rate dT/dt as, for instance, in Lasaga, Richardson and Holland (1977) and Wilson and Smith (1984). The results are not compatible with such a simple model, since a minimum cooling rate of 10° to 30°C my^{-1} is required to preserve growth profiles in the biggest garnet grains depending of the diffusion coefficient chosen, whereas a visible diffusion boundary layer at garnet rims indicates a maximum cooling rate of about 0.5° to 1°C

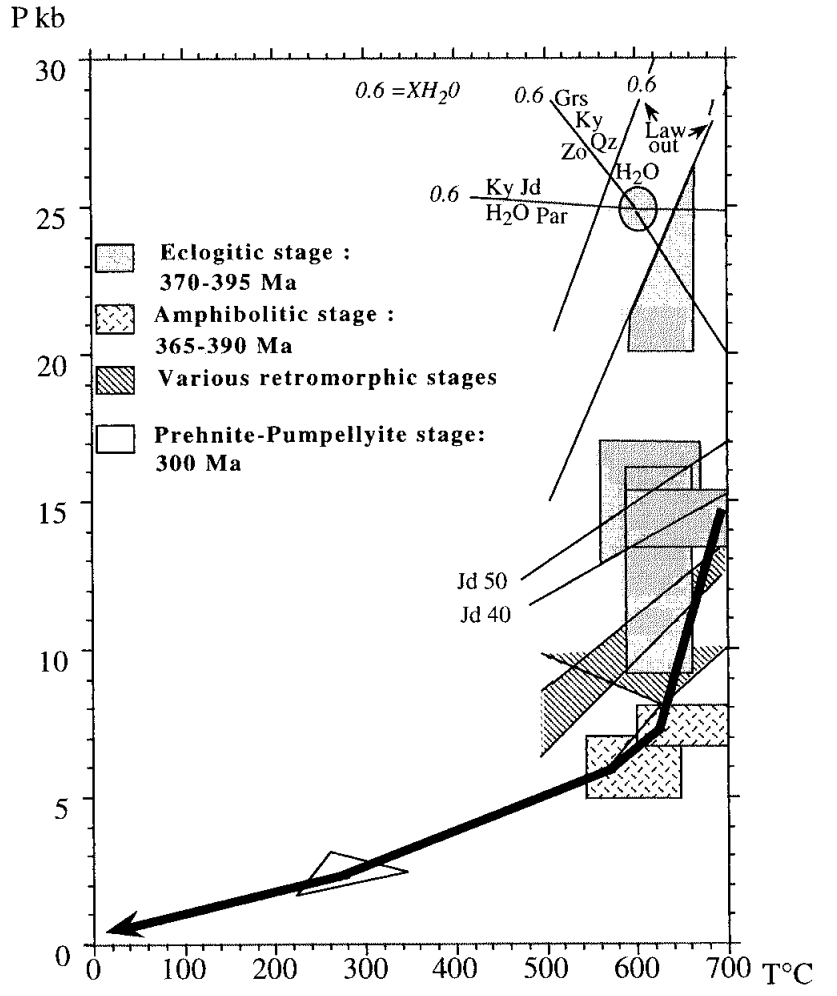

Fig. 9. The PTt path of the Münchberg eclogites (data from Gebauer and Grünenfelder, 1979; Söllner, Köhler, and Müller-Sohnius, 1981; Franz, Thomas, and Smith, 1986; Schüssler and others, 1986; Klemd, 1989; Kreuzer and Seidel, 1989; Kreutzer and others, 1989; Klemd, Matthes, and Okrusch, 1991; Hammerschmidt and Franz, 1992; O'Brien, 1993).

my^{-1}. We consider that this result reflects the inadequacy of the constant cooling rate assumption for metamorphic areas, in which temperature varies both in time and space. In consequence, we hereafter assume that the cooling rate actually decreases with time. A three-step history meant to fit the observed P-T path was constructed (1) by assuming that the sequence cooling rates is constrained by the preceding arguments on garnet zoning and (2) by choosing the break points in such a way that the middle PT segment overlaps with the observed PT path (fig. 9). A sequence of cooling rates decreasing from $-10°C\ my^{-1}$ during 7.5 my, to $-5°C\ my^{-1}$ during 10 my, and $-0.5°C\ my^{-1}$ to the cessation of diffusion, explains the observations reasonably well if the coefficient of Chakraborty and Ganguly (1992) is used. Growth zoning is preserved in garnets with a

radius in excess of 250 μm, while the smallest grains are homogenized. A zonation is observed at the garnet rims, with a suitable thickness of 30 μm for the boundary layer, but its amplitude is somewhat too small. If the data of Freer (1981) are used, the sequence of cooling rates must be changed into -30°C my^{-1} during 2.5 my, to -5°C my^{-1} during 10 my, and -1°C my^{-1} to the cessation of diffusion. The results are rather insensitive to a moderate change in the cooling rate during the intermediate stage. They are somewhat

TABLE 3

Temperature estimates on garnet-clinopyroxene pairs

Sample		rim T (°C)			core T (°C)		
		Ellis and Green	Råheim and Green	Krogh	Ellis and Green	Råheim and Green	Krogh
M10 site 2	1	705	663	663	712	657	671
	2	698	658	658	723	668	683
M8 site 1		661	610	610	687	655	636
M8 site 3		656	600	600	686	695	612
M8 site 7		698	651	651	733	668	697

The calculations were made using the rim concentration for clinopyroxene and either the rim (column 1) or core (column 2) concentration for garnet. The temperatures are based on Råheim and Green (1974), Ellis and Green (1979), and Krogh (1988) calibrations.

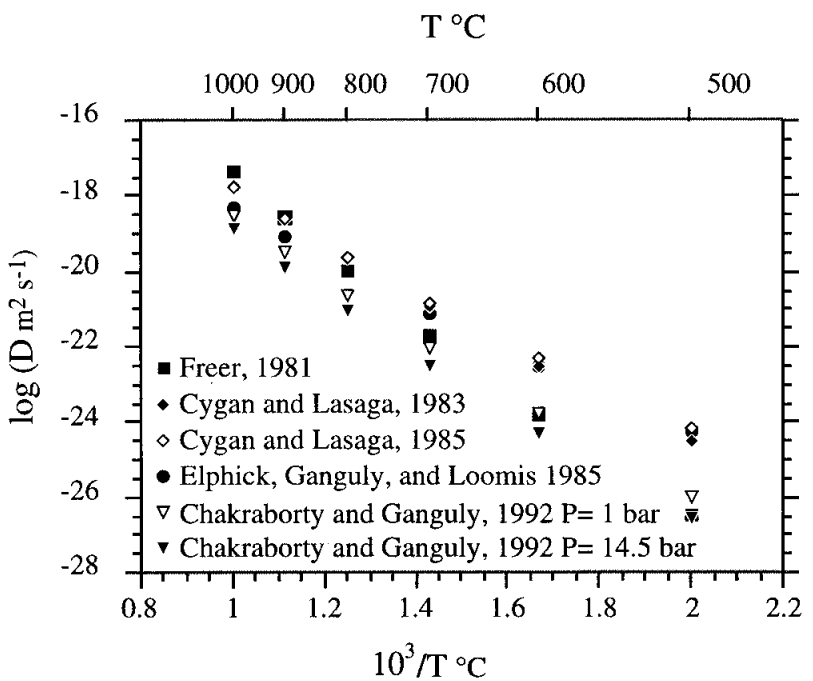

Fig. 10. Ahrrenius plot of the diffusion data sets from Freer (1981), Elphick et al. (1981), Cygan and Lasaga (1983), and Chakraborty and Ganguly (1992). The data from Chakraborty and Ganguly (1992) have been used with a garnet composition similar to that of the Münchberg samples and for two different pressures, 1 bar and 14.5 kb.

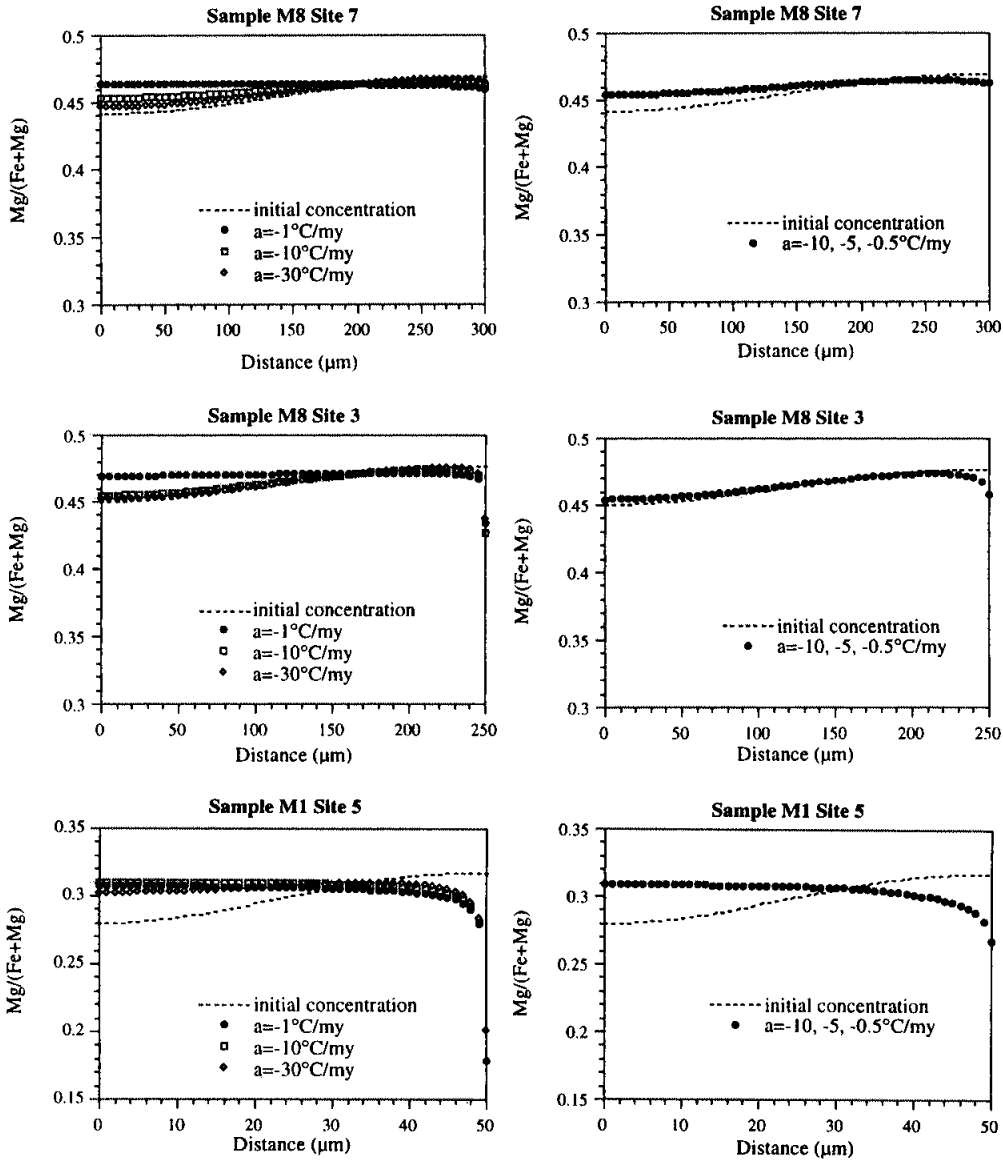

Fig. 11. Composition profiles in garnet simulated for a grain size and compositions similar to those measured in the Münchberg eclogites and plotted in figure 8. The garnet crystals are initially zoned. The initial temperatures are given by the composition of the clinopyroxene-garnet pair and range from 650° to 700°C (see text). (A) Diffusion coefficients are calculated from Chakraborty and Ganguly (1992). The profiles correspond to four sets of cooling rates: one stage for plots on the left, three stages for those on the right.

more sensitive to the duration of each step but the overall amplitude of cooling confines the timing of cooling rate discontinuities within narrow limits.

The difficulty in accounting for the amplitude of the zoning in the boundary layer may have several possible causes:

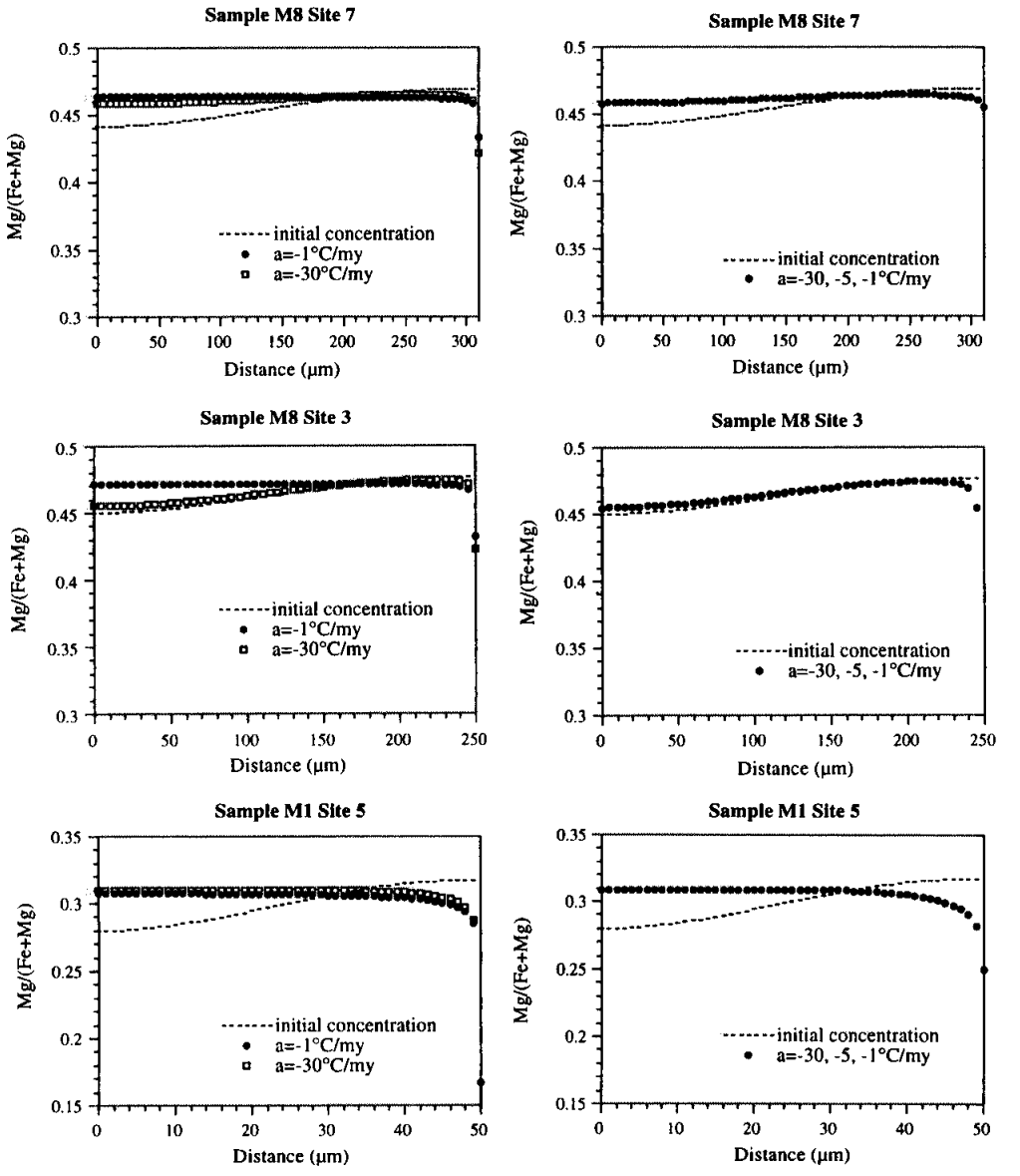

(B) Diffusion coefficients are calculated from Freer (1981). The profiles correspond to three sets of cooling rates: one stage for plots on the left, three stages for those on the right.

· The growth zoning (initial profile) is unknown which may bias the mass balance condition.

· The relative volumetric proportion of clinopyroxene and garnet involved in Fe-Mg exchange may be incorrectly estimated by the models. The distance over which intergranular diffusion is effective is poorly known and diffusion in pyroxene may be faster than what is estimated from Brady and MacAllister's (1983) data. The absence of visible zoning in eclogitic pyroxenes under 1000°C supports however a slow diffusion

rate. Although a larger clinopyroxene-garnet ratio would in principle result in a greater amplitude of zoning, it can be checked that this is not a significant effect.

· The temperature-time relations selected for the thermal history of the sample are not adequate. Most importantly, pervasive fluid transport and intergranular diffusion may not be continuous during the retrograde history. Although scattered and minute, symplectites represent evidence for circulating fluids and for the production of new mineral phases upon decompression into the amphibolite facies (O'Brien, 1993; Klemd, 1989) which biases the mass balance between garnet and clinopyroxene.

Pressure-time History and Exhumation Rates

The estimation of the pressure-time relation from the results derived in the temperature-time section demands that temperature is related to pressure through conventional thermobarometry (fig. 9). The temperature-time history can be translated into vertical exhumation rates v_z using

$$v_z = \frac{dz}{dt} = \frac{1}{\rho g}\frac{dP}{dT}\frac{dT}{dt}$$

where z stands for depth, g for the acceleration of gravity, and the value of density ρ is 3000 kg m^{-3}.

The condition that growth zoning is preserved has been shown to require a minimum cooling rate of -10 (-30 with Freer's data) my^{-1} in the high temperature part of the exhumation path where the minimum slope of the PT path is 0.05 kb $°C^{-1}$. Using these values, we get a minimum exhumation rate of 2 (5) mm yr^{-1}. The condition that the diffusion boundary layer is visible in garnets requires a maximum cooling rate of -0.5 (-1)°C my^{-1} in the low temperature part where the maximum slope of the PT path is 0.04 kb $°C^{-1}$. Using these values a maximum exhumation rate of 0.06 (0.13) mm yr^{-1} is inferred.

For the three-step PTt history that, in the previous section, was found to fit well the observed P-T path and the zoning patterns, the inferred exhumation rates decrease from an initial value of 3 (9) mm yr^{-1} at 14 kb to a value of 0.5 mm yr^{-1} after several my (fig. 12). Next to the surface, exhumation rate finally drops down to very small values of $\approx$0.02 (0.04) mm yr^{-1}. O'Brien's (1993) work on different rocks from the same area suggests, however, that the deepest pressure estimated by geobarometry (14 kb) on these samples is certainly a lower limit for the onset of exhumation. His pressure estimate of 25 kb would result, for a same initial temperature, in exhumation being initially much faster with rates in excess of 8 (24) mm yr^{-1}.

The sequence of exhumation velocities inferred from the zoned Münchberg garnets is compatible with independent evidence. First, the thermal boundary layer inferred from the PT diagram of figure 9 corresponds to approx 6 kb or 20 km. At steady-state, the thickness δ of the thermal boundary layer would be scaled by a thermal Peclet number $Pe = (\partial z/\partial t)\delta/\kappa \approx 1$, which for $\kappa = 25$ km^2 my^{-1} indicates a mean exhumation velocity of $\approx$1.25 mm yr^{-1}. Second, the high-temperature part of the exhumation path ($\approx$30 km) is confined within the errors of the geochronological measurements ($\approx$30 my, see above) which requires a minimum velocity of 1 mm yr^{-1}. The transfer to the prehnite pumpellyite facies ($\approx$15 km) is reached some 75 my later at a velocity of $\approx$0.2 mm yr^{-1}. Similar conclusions with comparable exhumation velocities were drawn for the Alps and the Massif Central of France by Duchêne, Lardeaux, and Albarède (1997, in press) from a review of PT and geochronological data.

Tectonic significance

A rock sample records the rate of change of the uplift velocity dv_z/dt with respect to a fixed reference frame such as sealevel for a point moving passively with the crust, which meets the lagrangian definition of movement. The lagrangian derivative dv_z/dt is related to the rate of change of the uplift velocity $\partial v_z/\partial$ t at a constant depth by (Batchelor, 1967):

$$\frac{dv_z}{dt} = \frac{\partial v_z}{\partial t} + V.\,\text{grad}\, v_z$$

where V is the displacement velocity. The vertical component of V is the uplift rate. In geological terms, dv_z/dt is the sum of a secular component $\partial v_z/\partial t$ and of a component

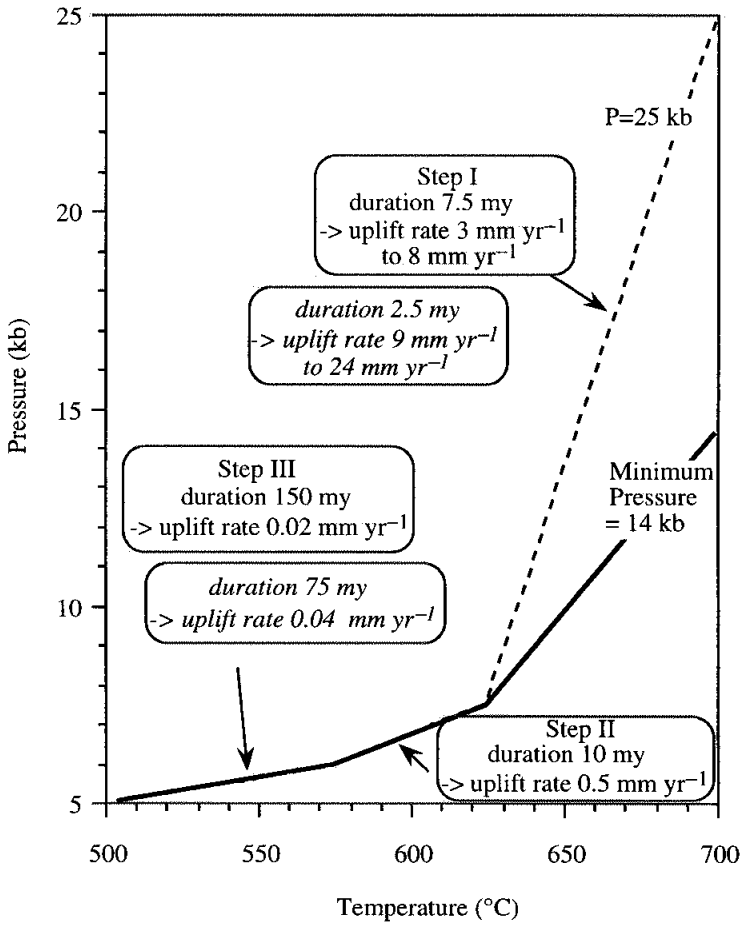

Fig. 12. Pressure-temperature-time history of the Münchberg eclogites as inferred from the zoning profiles. The uplift rates have been calculated using the PT path of figure 9. In plain text: the uplift rates correspond to the three stages used in the right part of fig. 11A, and result from the simulations made with the diffusion coefficient of Chakraborty and Ganguly (1992). In italic: the uplift rates correspond to the three stages used in the right part of fig. 11B and result from the simulations made with the diffusion coefficient of Freer (1981).

related to the rate of deformation. This second term is zero in any one-dimensional formulation of this equation. For a non-deformable crust, the term grad v_z is zero. The denudation rate (dv_z/dt) and the uplift velocity ($\partial v_z/\partial t$) must then be equal, especially in the high-temperature part of the PTt path where exhumation is fairly rapid (>5 mm yr^{-1}). Erosion rates in excess of 1 mm yr^{-1} have been locally observed (Li, 1976; Nie and others, 1994) but are uncommon over large areas and periods of time (Ahnert, 1970; Pinet and Souriau, 1988). A very significant fraction of the exhumation velocity dv_z/dt must therefore be accommodated by deformation in the crust. In order to preserve continuity, the flow lines must flatten near the surface thereby fulfilling the condition that the divergence of the velocity field (div V) is zero. This regime is essentially equivalent to that of the prism model (Cowan and Silling, 1978; Cloos, 1982; Platt, 1986; Allemand and Lardeaux, 1997). As in other areas where high-pressure rocks were rapidly brought to the surface, such as the Alps and the Massif Central of France, exhumation rates decreasing upward therefore would correspond to a regime of intense extension in the shallow parts of the orogenic domain. Near-surface extension around outcrops of high-pressure rocks is know from a variety of environments, including the Alps (Ballèvre, Merle and Lagabuella, 1990; Philippot, 1990; Michard, Chopin and Henry, 1993; Steck and Hunziker, 1994) and the Massif Central (Ménard and Molnar, 1988; Mattauer, Buinel and Matte, 1988; Malavieille and others, 1990; Faure, 1995) but still remains to be described for the Münchberg.

CONCLUSION

The numerical modeling of zoning patterns in eclogitic minerals suggests that long range intergranular transport is necessary to ensure the creation of a retrograde (diffusion) zoning patterns in garnets.

Diffusion zoning is expected in eclogitic garnets with climax temperature higher than 650°C. Concentration profiles will depend not only on the temperature evolution, but also on the microstructure, i.e. on the respective proportions of garnet and pyroxene.

The garnets from the Münchberg eclogites show both growth zoning in the biggest grains and a 30 μm diffusion boundary layer. The simultaneous presence of these two zoning patterns requires a multi-stage history with initial exhumation rates in excess of 5 mm yr^{-1} rapidly decreasing in a few million years.

The large value of exhumation rates at depth does not seem to be compensated by erosion which suggests a regime of intense extension in the shallow levels of the orogenic domain.

ACKNOWLEDGMENTS

We would like to express our thanks to Véronique Gardien and Eric Reusser for their help in analyzing the samples and for granting machine time. A review of an early draft by Patrick O'Brien and the comments from Sumit Chakraborty and another unidentified reviewer, were helpful.

APPENDIX A

In order to solve the diffusion eq (1), the radial coordinate axis in the garnet is divided into $m - 1$ intervals Δr ($m - n - 1$ in clinopyroxene) and the time axis into an arbitrary number of intervals Δt such that $r = (i - 1)\Delta r$ with $i = 1, \ldots m$, and $t = j\Delta t$ with $j = 0, 1, \ldots$ (fig. A1). The spatial derivatives are replaced by centered differences while a backward difference is used for the time derivatives such that

$$\frac{C_{i,j} - C_{i,j-1}}{\Delta t} = D_{Grt}\left(\frac{2}{r} \times \frac{C_{i+1,j} - C_{i-1,j}}{2\Delta r} + \frac{C_{i+1,j} - 2C_{i,j} + C_{i-1,j}}{\Delta r^2}\right) \quad \text{(A1)}$$

where $C_{i,j}$ represents the concentration Mg/(Fe+/Mg) at the node defined by $i\Delta r$ and $j\Delta t$. Successive concentration profiles are calculated from the initial distribution for increasing j. In both models, eq (1) is

expressed for garnet as

$$\frac{C_{i,j}^{Grt} - C_{i,j-1}^{Grt}}{\Delta t} = D_{Grt}\left(\frac{2}{(i-1)\Delta r_{Grt}} \times \frac{C_{i+1,j}^{Grt} - C_{i-1,j}^{Grt}}{2\Delta r_{Grt}} + \frac{C_{i+1,j}^{Grt} - 2C_{i,j}^{Grt} + C_{i-1,j}^{Grt}}{\Delta r_{Grt}^2}\right) \quad \text{(A2A)}$$

Eq (1) for pyroxene reads

$$\frac{C_{i,j}^{Cpx} - C_{i,j-1}^{Cpx}}{\Delta t} = D_{Cpx}\left(\frac{2}{R_{Grt} + (i-n)\Delta r_{Cpx}} \times \frac{C_{i+1,j}^{Cpx} - C_{i-1,j}^{Cpx}}{2\Delta r_{Cpx}} + \frac{C_{i+1,j}^{Cpx} - 2C_{i,j}^{Cpx} + C_{i-1,j}^{Cpx}}{\Delta r_{Cpx}^2}\right) \quad \text{(A2B)}$$

for model I and

$$\frac{C_{i,j}^{Cpx} - C_{i,j-1}^{Cpx}}{\Delta t} = D_{Cpx}\left(\frac{2}{(m-i)\Delta r_{Cpx}} \times \frac{C_{i+1,j}^{Cpx} - C_{i-1,j}^{Cpx}}{2\Delta r_{Cpx}} + \frac{C_{i+1,j}^{Cpx} - 2C_{i,j}^{Cpx} + C_{i-1,j}^{Cpx}}{\Delta r_{Cpx}^2}\right) \quad \text{(A2C)}$$

for model II. Defining $\alpha_{Grt} = D_{Grt}\,\Delta t/\Delta r_{Grt}^2$, $\alpha_{Cpx} = D_{Cpx}\,\Delta t/\Delta r_{Cpx}^2$, and extracting $C_{i,j-1}$ from (A2A-C), we get the three corresponding equations

$$-\alpha_{Grt}\left(1 - \frac{1}{i-1}\right) C_{i-1,j}^{Grt} + (1 + 2\alpha_{Grt})\, C_{i,j}^{Grt} - \alpha_{Grt}\left(1 + \frac{1}{i-1}\right) C_{i+1,j}^{Grt} = C_{i,j-1}^{Grt} \quad \text{(A3A)}$$

$$-\alpha_{Cpx}\left(1 - \frac{1}{\frac{R_{Grt}}{\Delta r_2} + i - n}\right) C_{i-1,j}^{Cpx} + (1 + 2\alpha_{Cpx})\, C_{i,j}^{Cpx} - \alpha_{Cpx}\left(1 + \frac{1}{\frac{R_{Grt}}{\Delta r_2} + i - n}\right) C_{i+1,j}^{Cpx} = C_{i,j-1}^{Cpx} \quad \text{(A3B)}$$

$$-\alpha_{Cpx}\left(1 - \frac{1}{m-i}\right) C_{i-1,j}^{Cpx} + (1 + 2\alpha_{Cpx})\, C_{i,j}^{Cpx} - \alpha_{Cpx}\left(1 + \frac{1}{m-i}\right) C_{i+1,j}^{Cpx} = C_{i,j-1}^{Cpx} \quad \text{(A3C)}$$

Four boundary conditions (two per mineral) are needed to solve the two sets of partial differential equations:

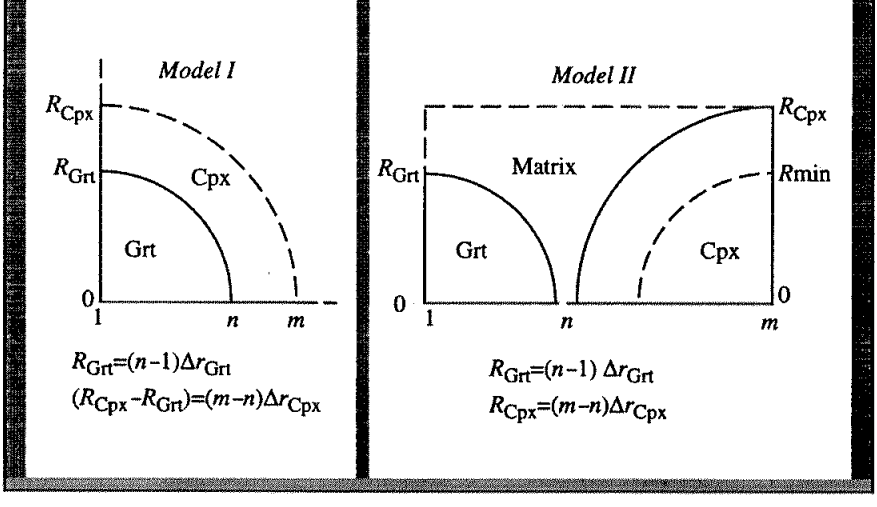

Fig. A1. Left: Inclusion Model I. Right: Population Model II. Concentrations are assumed to be homogeneous within the sphere of radius Rmin.

–The no-flux condition at the center of the garnet grain ($r = 0, i = 1$) is expressed using a fictitious point at $i = 0$. Once this condition is inserted into (A2A), we get

$$-2\alpha_1 C^{Grt}_{2,j} + (1 + 2\alpha_1) C^{Grt}_{1,j} = C^{Grt}_{1,j-1} \tag{A4}$$

–The clinopyroxene boundary layer is very thin with respect to the grain radius. In order to minimize computational effort, the calculation is restricted to the rim affected by diffusion and the no-flux condition replaced by is $C_{k,j} = C_{k,j-1}$ at any convenient node k located well outside the boundary layer.

–The last two boundary conditions for the contact between the two minerals at $i = n$ cannot be formulated explicitly. Concentrations at the surface of each mineral are derived by expressing first the equilibrium condition (2) at the interface which reads

$$K_D = \frac{C^{Grt}_{Fe}}{C^{Grt}_{Mg}} \times \frac{C^{Cpx}_{Mg}}{C^{Cpx}_{Fe}} = \frac{1 - C^{Grt}_{Mg}}{C^{Grt}_{Mg}} \times \frac{C^{Cpx}_{Mg}}{1 - C^{Cpx}_{Mg}} \tag{A5}$$

The second condition expresses mass conservation during exchange

$$P_{Grt} D_{Grt} \frac{C^{Grt}_{n+1,j} - C^{Grt}_{n-1,j}}{\Delta r_{Grt}} - P_{Cpx} D_{Cpx} \frac{C^{Cpx}_{n+1,j} - C^{Cpx}_{n-1,j}}{\Delta r_{Cpx}} = 0 \tag{A6}$$

for model I and model II, respectively, and where P is the volume fraction of Fe + Mg times the total surface of exchange of each mineral phase. We use one more time fictitious points $C^{Grt}_{n+1,j}$ and $C^{Cpx}_{n-1,j}$ which are eliminated using eq (A2) at $i = n$ giving, for model I

$$\begin{aligned}
&-2\alpha_{Grt}\alpha_{Cpx} C^{Grt}_{n-1,j} + \alpha_{Cpx}(1 + 2\alpha_{Grt}) C^{Grt}_{n,j} \\
&+\alpha_{Grt}(1 + 2\alpha_{Cpx}) \frac{D_{Cpx}}{D_{Grt}} \frac{\Delta r_{Grt}}{\Delta r_{Cpx}} \frac{n}{n-1} \frac{R_{Grt}}{R_{Grt} - \Delta r_{Cpx}} C^{Cpx}_{n,j} \\
&-2\alpha_{Grt}\alpha_{Cpx} \frac{D_{Cpx}}{D_{Grt}} \frac{\Delta r_{Grt}}{\Delta r_{Cpx}} \frac{n}{n-1} \frac{R_{Grt}}{R_{Grt} - \Delta r_{Cpx}} C^{Cpx}_{n+1,j} \\
&= \alpha_{Cpx} C^{Grt}_{n,j-1} + \alpha_{Grt} \frac{D_{Cpx}}{D_{Grt}} \frac{\Delta r_{Grt}}{\Delta r_{Cpx}} \frac{n}{n-1} \frac{R_{Grt}}{R_{Grt} - \Delta r_{Cpx}} C^{Cpx}_{n,j-1}
\end{aligned} \tag{A7A}$$

and for model II

$$\begin{aligned}
&-2 P_{Grt}\alpha_{Grt} \frac{n-1}{n} C^{Cpx}_{n-1,j} \\
&+ P_{Grt} \frac{n-1}{n} (1 + 2\alpha_{Grt}) C^{Grt}_{n,j} + P_{Cpx} \frac{\Delta r_{Cpx}}{\Delta r_{Grt}} \left(\frac{R_{Cpx}}{R_{Grt}}\right)^2 \frac{m-n}{m-n-1} (1 + 2\alpha_{Cpx}) C^{Cpx}_{n,j} \\
&-2 P_{Cpx}\alpha_{Cpx} \frac{\Delta r_{Cpx}}{\Delta r_{Grt}} \left(\frac{R_{Cpx}}{R_{Grt}}\right)^2 \frac{m-n}{m-n-1} C^{Cpx}_{n+1,j} \\
&= P_{Grt} \frac{n-1}{n} C^{Grt}_{n,j-1} + P_{Cpx} \frac{\Delta r_{Cpx}}{\Delta r_{Grt}} \left(\frac{R_{Cpx}}{R_{Grt}}\right)^2 \frac{m-n}{m-n-1} C^{Cpx}_{n,j-1}
\end{aligned} \tag{A7B}$$

In rows $n - 1$, n, and $n + 1$, $C^{Cpx}_{n,j}$ is expressed with respect to $C^{Grt}_{n,j}$ using eq (A5).

Eqs (A3A), (A3B), (A4), and (A7A) are combined into one single matrix equation for model I, and likewise eqs (A3A), (A3C), (A4), and (A7B) for model II, in the form $M_j C_j = C_{j-1}$ with M_j being a time-dependent $k \times k$ matrix and C_j being the k-column vector of concentrations at step j. Because of the non-linearity of the boundary condition, this matrix equation is solved iteratively by the Newton-Raphson method. The step $j - 1$ provides a good initial estimate which normally ensures a very fast convergence.

REFERENCES

Ahnert, F., 1970, Functional relationships between denudation, relief, and uplift in large mid-latitude drainage basins: American Journal of Science, v. 268, p. 243–263.

Allemand, P., and Lardeaux, J.-M., 1997, Strain partitioning and metamorphism in a deformable orogenic wedge: application to the Alpine Belt: Tectonophysics, v. 280, p. 157–170.

Anderson, D. E., and Buckley, G. R., 1973, Zoning in garnet: diffusion models: Contributions to Mineralogy and Petrology, v. 40, p. 87–104.

Ballèvre, M., Merle, O., and Lagabrielle, Y., 1990, Tertiary ductile normal faulting as a consequence of lithospheric stacking in the Western Alps: Mémoires de la Société Géologique de France, v. 156, p. 227–236.

Batchelor, G. K., 1967, Fluid dynamics: Cambridge, United Kingdom, Cambridge University Press.

Behr, H. J., Engel, W., and Franke, W., 1982, Variscan wildflysch and nappe tectonics in the Saxothuringian zone (Northeast Bavaria, West Germany): American Journal of Science, v. 282, p. 1438–1470.

Bocchio, R., 1995, Chemical variations in clinopyroxene and garnet from eclogites of the Vara Valley (Voltri Group, Italy): European Journal of Mineralogy, v. 7, p. 103–117.

Brady, J. B., and Mac Allister, R. H., 1983, Diffusion data for clinopyroxenes from homogeneization and self-diffusion experiments: American Mineralogist, v. 68, p. 95–105.

Buatier, M., van Roermund, H. L. M., Drury, M. R., and Lardeaux, J.-M., 1991, Deformation and recristallisation mechanisms in naturally deformed omphacites from the Sesia-Lanzo zone; geophysical consequences: Tectonophysics, v. 195, p. 11–27.

Chakraborty, S., and Ganguly, J., 1992, Cation diffusion in aluminosilicate garnets:experimental determination in spessartine-almandine couples, evaluation of effective binary diffusion coefficients, and applications: Contributions to Mineralogy and Petrology, v. 111, p. 74–96.

Chakraborty, S., and Rubie, D. C., 1996, Mg tracer diffusion in aluminosilicate garnets at 750–850°C, 1 atm. and 1300°C, 8.5 GPa: Contributions to Mineralogy and Petrology, v. 122, p. 406–414.

Cloos, M., 1982, Flow melanges: Numerical modeling and geologic constraints on their origin in the Franciscan subduction complex, California: Geological Society of America Bulletin, v. 93, p. 330–345.

Cowan, D. S., and Silling, R. M., 1978, A dynamic model of accretion at trenches and its implications for the tectonic evolution of subduction complexes: Journal of Geophysical Research, v. 83, p. 5389–5396.

Crank, J., 1975, The Mathematics of diffusion (2nd edition): Oxford, Clarendon Press, p. 414.

Cygan, R. T., and Lasaga, A. C., 1983, Self-diffusion of magnesium in garnet at 750–900°C: Geological Society of America Abstracts with Programs, v. 15, p. 552.

——— 1985, Self diffusion of magnesium in garnet at 750° to 900°C.: American Journal of Science, v. 285, p. 328–350.

Darken, L. S., 1948, Diffusion, mobility and their interrelation through free energy in binary metallic systems.: American Institute of Mining and Metallurgical Engineers Transactions, v. 174, p. 184–194.

Dodson, M. H., 1973, Closure Temperature in cooling geochronological and petrological systems: Contributions to Mineralogy and Petrology, v. 40, p. 259–274.

Duchêne, S., Lardeaux, J.-M., and Albarède, F., 1997, Exhumation of eclogites: insight from retrograde depth-time path analysis: Tectonophysics, v. 280, p. 125–140.

Dudek, A., and Fediuková, E., 1974, Eclogites of the Bohemian Moldanubicum: Neues Jahrbuch für Mineralogie, Abhandlungen, v. 121, p. 127–159.

Eiler, J. M., Baumgartner, L. P., and Valley, J. W., 1992, Intercrystalline stable isotope diffusion: a fast grain boundary model: Contributions to Mineralogy and Petrology, v. 112, p. 543–557.

Ellis, D. J., and Green, D. H., 1979, An experimental study of the effect of Ca upon garnet-clinopyroxene Fe-Mg exchange equilibria: Contributions to Mineralogy and Petrology, v. 71, p. 13–22.

Elphick, S. C., Ganguly, J., and Loomis, T. P., 1981, Experimental study of Fe-Mg interdiffusion in aluminosilicate garnet: American Geophysical Union Transactions (EOS), v. 62, p. 411.

——— 1985, Experimental determination of cation diffusivities in aluminosilicate garnets I Experimental methods and interdiffusion data: Contributions to Mineralogy and Petrology, v. 90, p. 36–44.

Erambert, M. and Austreim, H., 1993, The effect of fluid and deformation on zoning patterns in polymetamorphic garnets: Contributions to Mineralogy and Petrology, v. 115, p. 204–214.

Evans, B. W., 1965, Microprobe study of zoning in eclogite garnets: Geological Society of America Special Paper, v. 87, p. 54.

Faure, M., 1995, Late orogenic carboniferous extensions in the Variscan French Massif Central: Tectonics, v. 14, p. 132–153.

Franke, W., 1984, Variszischer Deckenbau im Raum der Münchberger Gneissmasse-abgeleitet aus der Fazies, Deformation und Metamorphose im umgebenden Paleozoïkum: Geotektonische Forschungen, v. 68, p. 1–253.

Franz, G., Thomas, S., and Smith, D. C., 1986, High-pressure phengite decomposition in the Weissenstein eclogite, Münchberger Gneiss Massif, Germany: Contributions to Mineralogy and Petrology, v. 92, p. 71–85.

Freer, R., 1981, Diffusion in Silicate Minerals and Glasses: A Data Digest and a Guide to Literature: Contributions to Mineralogy and Petrology: v. 76, p. 440–454.

Gebauer, D., and Grünenfelder, M., 1979, U-Pb zircon and Rb-Sr mineral dating of eclogites and their country rocks. example:Münchberg Massif, Northern Bavaria: Earth and Planetary Science Letters, v. 42, p. 35–44.

Ghent, E. D., 1988, A review of chemical zoning in eclogite garnets, in Smith, D. C., editor, Eclogites and eclogite-facies rocks: Elsevier, Amsterdam, Netherlands, p. 207–236.

Giletti, B. J., 1986, Diffusion effects on oxygen isotope temperatures of slowly cooled igneous and metamorphic rocks: Earth and Planetary Science Letters, v. 77, p. 218–228.
Green, T. H., and Helmann, L., 1982, Fe-Mg partitioning between coexisting garnet and phengite at high pressure, and comments on a garnet-phengite geothermometer: Lithos, v. 15, p. 253–266.
Griffin, W. L., 1987, 'On the eclogites of Norway'–65 years later: Mineralogical Magazine, v. 51, p. 333–343.
Hammerschmidt, K., and Franz, G., 1992, Retrograde evolution of eclogites: evidence from microstructures and 40Ar/39Ar white mica dates, Münchberg Massif, Northern Bavaria: Contribution to Mineralogy and Petrology, v. 111, p. 113–125.
Hollister, L. S., 1966, Garnet zoning: an interpretation based on the Rayleigh fractionation model: Science, v. 154, p. 1647–1651.
Jamveit, B., 1987, Metamorphic evolution of the Eiksunddal eclogite complex, Western Norway, and some tectonic implications: Contributions to Mineralogy and Petrology, v. 95, p. 82–99.
Jenkin, G. R. T., Farrow, C. M., Fallick, A. E., and Higgins, D., 1994, Oxygen isotope exchange and closure temperatures in cooling rocks: Journal of Metamorphic Geology, v. 12, p. 221–236.
Jiang, J., and Lasaga, A. C., 1990, The effect of post-growth thermal events on growth-zoned garnet: implications for metamorphic P.T. history calculations: Contributions to Mineralogy and Petrology, v. 105, p. 454–459.
Kienast, J. R., Lombardo, B., Biino, G., and Pinardon, J. L., 1991, Petrology of the very-high-pressure eclogitic rocks from the Brossasco-Isasca complex, Dora Maira Massif, Italian Western Alps: Journal of Metamorphic Geology, v. 9, p. 19–34.
Klemd, R., 1989, P-T evolution and fluid inclusion caracteristics of retrograded eclogites, Münchberg Gneiss Complex, Germany: Contributions to Mineralogy and Petrology, v. 102, p. 221–229.
Klemd, R., Matthes, S., and Okrusch, M., 1991a, High-pressure relics in meta-sediments intercalated with the Weissenstein eclogite, Münchberg Gneiss Complex, Bavaria: Contributions to Mineralogy and Petrology, v. 107, p. 328–342.
Kretz, R., 1974, Some models for the rate of cristallization of garnet in metamorphic rocks: Lithos, v. 7, p. 123–131.
Kreuzer, H., and Seidel, E., 1989, Diskrete früh-devonische Ar/Ar Alter der Hangendserie (Münchberger Masse): Beiheft zum European Journal of Mineralogy, v. 1, p. 103.
Kreuzer, H., Seidel, E., Schüssler, U., Okrusch, M., Lenz, K. L., and Raschka, H., 1989, K-Ar geochronology of different tectonic units at the northwestern margin of the Bohemian Massif: Tectonophysics, v. 157, p. 149–178.
Krogh, E. J., 1988, The garnet-clinopyroxene Fe-Mg geothermometer–a reinterpretation of existing experimental data: Contributions to Mineralogy and Petrology, v. 99, p. 44–48.
Lardeaux, J. M., Caron, J. M., Nisio, P., Pequinot, G., and Boudeulle, M., 1986, Microstructural criteria for reliable thermometry in low-temperature eclogites: Lithos, v. 19, p. 187–203.
Lasaga, A. C., Richardson, S. M., and Holland, H. D., 1977, The mathematics of cation diffusion and exchange between silicate minerals during retrograde metamorphism., *in* Saxena, S. K., and Bhattacharji, S., editor, Energetics of Geological Process: Springer Verlag, New York, p. 353–388.
Li, Y.-H., 1976, Denudation of Taïwan Island since the Pliocene Epoch: Geology, v. 4, p. 105–107.
Malavieille, J., Guihot, P., Costa, S., Lardeaux, J.-M., and Gardien, V., 1990, Collapse of the thickened variscan crust in the French Massif Central: Mont Pilat extensional shear zone and St Etienne Late Carboniferous basin: Tectonophysics, v. 177, p. 139–149.
Mattauer, M., Brunel, M., and Matte, P., 1988, Failles Normales ductiles et grands chevauchements: une nouvelle analogie entre l'Himalaya et la chaîne hercynienne du Massif Central Français: Compte-rendu de l'Académie des Sciences de Paris, v. 306, p. 671–676.
Medaris, G., Jelínek, E., and Mísař, Z., 1995, Czech eclogites: Terrane settings and implications for the Variscan tectonic evolution of the Bohemian Massif: European Journal of Mineralogy, v. 7, p. 7–28.
Medaris, L. G., and Wang, H. F., 1986, A thermal tectonic model for high pressure rocks in the Basal Gneiss complex of Western Norway: Lithos, v. 19, p. 299–315.
Menard, G., and Molnar, P., 1988, Collapse of a Hercynian Tibetan Plateau into a late Paleozoic European Basin and Range Province: Nature, v. 334, p. 235–237.
Michard, A., Chopin, C., and Henry, C., 1993, Compression versus extension in the exhumation of the Dora-Maira coesite-bearing unit, Western Alps, Italy: Tectonophysics, v. 221, p. 173–193.
Nie, S., Yin, A., Rowley, D. B., and Jin, Y., 1994, Exhumation of the Dabie Shan ultra high pressure rocks and accumulation of the Songpan-Ganzi flysch sequence, central China: Geology, v. 22, p. 999–1002.
O'Brien, P. J., 1993, Partially retrograded eclogites of the Münchberg Massif, Germany: records of a multi-stage Variscan uplift history in the Bohemian Massif: Journal of Metamorphic Geology, v. 11, p. 241–260.
Pattison, D. R. M., and Bégin, J., 1994, Zoning pattern in orthopyroxene and garnet in granulites: implications for geothermometry: Journal of Metamorphic Geology, v. 12, p. 387–410.
Philippot, P., 1990, Opposite vergence of nappes and crustal extension in the French-Italian Western Alps: Tectonics, v. 9, p. 1143–1164.
Pinet, P., and Souriau, M., 1988, Continental erosion and large-scale relief: Tectonics, v. 7, p. 563–582.
Platt, J. P., 1986, Dynamics of orogenic wedges and the uplift of high pressure metamorphic rocks: Geological Society of America Bull, v. 97, p. 57–71.
Råheim, A., and Green, D. H., 1974, Experimental determination of the temperature and pressure dependence of the Fe-Mg partition coefficient for coexisting garnet and clinopyroxene: Contributions to Mineralogy and Petrology, v. 48, p. 179–203.
Sautter, V., and Harte, B., 1990, Diffusion gradients in an eclogite xenolith from the Roberts Victor kimberlite pipe: (2) kinetics and implications for petrogenesis: Contributions to Mineralogy and Petrology, v. 105, p. 637–649.

Schüssler, U., Oppermann, U., Kreuzer, H., Seidel, E., Okrusch, M., Lenz, K. L., and Raschke, H., 1986, Zur Alterstellung der ostbayrischen Kristallins. Ergebnisse neuer K-Ar Datierungen: Geologica Bavarica, v. 89, p. 21–47.

Smith, D. C., and Wilson, C. R., 1985, Garnet-olivine equilibration during cooling in the mantel: American Mineralogist, v. 70, p. 30–39.

Smith, D. C., Kienast, J. R., Kornprobst, J., and Lasnier, B., 1982, Eclogites and their problems: an introduction to the First International Eclogite Conference (F.I.E.C.): Terra Cognita, v. 2, p. 283–295.

Söllner, F., 1978, Rb-Sr Altersbestimmungen an Mineralen end Gesteinen der Münchberger Gneismasse: ms, Ph.D. thesis, University of Munich.

Söllner, F., Köhler, H., and Müller-Sohnius, D., 1981, Rb-Sr Altersbestimmungen an Gesteinen der Münchberger Gneismasse (MM) NE-Bayern. Teil 1, Gesamtgesteinsdatierungen: Neues Jahrbuch für Mineralogie, Abhandlungen, v. 141, p. 90–112.

Spear, F. S., and Selverstone, J., 1983, Quantitative P-T Paths from zoned minerals: Theory and Applications: Contributions to Mineralogy and Petrology, v. 83, p. 348–357.

Steck, A., and Hunziker, J. C., 1994, The tertiary structural and thermal evolution of the Central Alps. Compressional and extensional structures in an orogenic belt: Tectonophysics, v. 238, p. 229–254.

Stosch, H. G., and Lugmair, G. W., 1990, Geochemistry and evolution of MORB-type eclogites from the Münchberg Massif, southern Germany: Earth and Planetary Science Letters, v. 99, p. 230–249.

Tracy, R. J., 1982, Compositional zoning and inclusions in metamorphic minerals, in Ferry, J. M., editor, Caracterization of metamorphism through mineral equilibria: Mineralogical Society of America, p. 355–393.

Van Roermund, H. L. M., and Boland, J. N., 1981, The dislocation structures of naturally deformed eclogites: Tectonophysics, v. 78, p. 403–418.

Wilson, C. R., and Smith, D., 1984, Cooling rate estimates from mineral zonation: resolving power and applications: International Kimberlite Conference, Third, Proceedings, v. 2, p. 265–276.